Packet Size Optimization for Multiple Input Multiple Output Cognitive Radio Sensor Networks aided Internet of Things.

Chitradeep Majumdar*, Doohwan Lee†, Aaqib Ashfaq Patel*, S. N. Merchant*, U. B. Desai ‡
*IIT Bombay, † RCAST, The University of Tokyo, ‡ IIT Hyderabad
email: cm6v07@ee.iitb.ac.in, leedh@mlab.t.u-tokyo.ac.jp, aaqib@ee.iitb.ac.in, merchant@ee.iitb.ac.in, ubdesai@iith.ac.in

***Abstract*—The determination of Optimal Packet Size (OPS) for Cognitive Radio assisted Sensor Networks (CRSNs) architecture is non-trivial. State of the art in this area describes various complex techniques to determine OPS for CRSNs. However, it is observed that under high interference from the surrounding users, it is not possible to determine a feasible optimal packet size of data transmission under the simple point-to-point CRSN network topology. This is contributed primarily due to the peak transmit power constraint of the cognitive nodes. To address this specific challenge, this paper proposes a Multiple Input Multiple Output based Cognitive Radio Sensor Networks (MIMO-CRSNs) architecture for futuristic technologies like Internet of Things (IoT) and machine-to-machine (M2M) communications. A joint optimization problem is formulated taking into account network constraints like the overall end to end latency, interference duration caused to the non-cognitive users, average BER and transmit power. We propose our Algorithm-1 based on generic exhaustive search technique blue to solve the optimization problem. Furthermore, a low complexity suboptimal Algorithm-2 based on solving classical Karush-Kuhn-Tucker (KKT) conditions is proposed. These algorithms for MIMO-CRSNs are implemented in conjunction with two different channel access schemes. These channel access schemes are Time Slotted Distributed Cognitive Medium Access Control denoted as MIMO-DTS-CMAC and CSMA/CA assisted Centralized Common Control Channel based Cognitive Medium Access Control denoted as MIMO-CC-CMAC. Simulations reveal that the proposed MIMO based CRSN network outperforms the conventional point-to-point CRSN network in terms of overall energy consumption. Moreover, the proposed Algorithm-1 and Algorithm2 shows perfect match and the implementation complexity of Algorithm-2 is much lesser than Algorithm-1. Algorithm-1 takes almost 680 ms to execute and provides OPS value for a given number of users while Algorithm-2 takes 4 to 5 ms on an average to find the optimal packet size for the proposed MIMO-CRSN framework.**

***Index Terms*—Optimal packet size, cognitive radio sensor networks, energy-efficiency, quadrature amplitude modulation, convex optimization, medium access control.**

I. Introduction

COGNITIVE Radio (CR) has emerged as one of the most blue sought topic for research in the area of wireless communication over the past few years. Considering the exponential rise in the number of mobile phone users in the last decade, it was imperative to come up with a robust technology which would suffice this ever increasing need. The opportunistic spectrum utilization feature of cognitive radio was envisaged to be a promising solution to deal with this challenge [1]. Over the years as the CR technology evolved, the inherent challenges associated with this technology became more and more evident. Various network paradigms based on CR and its variants have been extensively explored by the researchers [2]. Furthermore, it became clear that CR technology which was primarily aimed for mobile communication can now be extended to other upcoming communication paradigms like Internet of Things (IoT) and Machine-to-Machine communications which are likely to be a part of the future wireless communication standards like LTE-A and 5G [3], [4]. These futuristic paradigms like IoT operates on the fundamental principle of data sensing, data acquisition and reliable data transmission from our physical surroundings to a remote processing unit which would process the received data and provide us with some useful information which improves our daily life. This typically involves large number of sensor nodes that continuously gather raw data from different applications. The pervasiveness, scalability of these nodes in terms of its number and the requisite for seamless reliable data transfer makes an IoT application somewhat distinct from the conventional wireless sensor network. These sensor nodes are often subjected to operational limitations like power constraint, limited coverage area and interference from other services coexisting the same frequency band. This motivated researchers to adapt the CR technology into conventional sensor network architecture to come up with Cognitive Radio based Sensor Networks (CRSNs) which could support the demand for IoT based applications in a more efficient way [5], [6]. In this paper we define cognitive nodes or secondary users as the users which have the cognitive channel sensing and switching capabilities whereas the sensor nodes which are not equipped with this cognitive feature or any other services operating within the same frequency band are coined as non-cognitive users.

This paper proposes a novel technique to determine the optimal packet size for a MIMO based CRSN architecture denoted as MIMO-CRSN. The motivation for data transmission with optimal packet size is clearly established by considering the tradeoff due to the overhead energy consumed due to retransmissions and the latency due to the transmission of

Dr. Doohwan Lee is presently working with NTT Network Innovation Laboratories, Yokosuka, Japan

the redundant bits like header and trailer present in a digital data packet. Optimal packet size determination in conventional sensor networks for both uncoded and coded systems were initially proposed in [7]. The authors of [8] proposed a technique to determine the optimal packet size for smart grids using conventional sensor networks. Measurements based on pathloss were obtained to characterize the channel in real time for the smart grid environment. Furthermore, this concept of OPS determination was further extended into CRSNs by the authors in [9] where the sensor nodes with cognitive radio features adapt their packet size dynamically depending on the network condition and other constraints like delay and interference duration to primary users. This was followed with few key literatures in this area like [10] where the authors proposed a dynamic packet optimization and channel selection scheme based on constrained Markov decision process. Majority of the work available in this area emphasizes on the optimization problem formulation to determine the optimal packet size (OPS) and an overview to solve the optimization problem. However the proposed optimization problems are, in general NP hard by nature requiring complex algorithms to solve them. This is not suitable for the sensor nodes which has a very limited computational capacity. To address this challenge we have proposed low complexity suboptimal algorithm in [11] for point-to-point CRSN architecture. We have analyzed the performances of the proposed algorithms based on their required execution time. However, it was observed that with increasing interference from the surroundings or non-cognitive users (-10 dB or more), feasible optimal packet size cannot be obtained due to the network constraints. The main reason for this is the peak power constraint for each individual sensor node of not transmitting beyond 100 mW transmit power. To overcome this challenge, we extend the concept from our previous work and propose a new paradigm based on Multiple Input Multiple Output (MIMO) based CRSNs.

The authors of [12], [13] and [14] have proposed the concept of MIMO based conventional sensor network architecture. The extensive simulation results have revealed significant improvement in the performance of the system in terms of overall energy consumption, transmission range and latency as compared to point-to-point system because MIMO technology enables to exploit diversity and array gain either at the transmitter / receiver end or both. Furthermore, in order to implement a simple MIMO based sensor network architecture when standard space time encoding strategies like Alamouti encoding scheme is applied, the overall transmit power required to attain a specific bit error rate threshold at the receiver end gets divided among the transmit antennas involved in MIMO mode of transmission. This is one of the important motivating factor to incorporate MIMO within the CRSN framework. However, the performance of the conventional MIMO based sensor network architecture when used simultaneously with the cognitive radio framework has not been explored in details. Therefore, exact quantification of the improved performance in terms of overall energy consumption, end-to-end delay and other relevant performance metrics needs to be evaluated and established. Operational criterions like overheads caused due to local intracluster information exchange to form virtual MIMO antenna array, channel sensing, handoff etc. needs to be taken into account. The concept of MIMO technology in general, is applied to enhance the overall throughput of the system by exploiting the diversity and array gain. There are few literatures available like [15] where the authors have coupled this MIMO technology along with an optimal packet size mode of transmission for a single base station with multiple antennas to establish an improved performance in terms of latency, throughput and energy-efficiency. Rate adaption with variable rate m-QAM modulation scheme was adopted as well. However, contribution of this work is mainly aimed towards mobile communication. For MIMO assisted wireless sensor network architecture, the overhead energy consumed due to the cluster formation needs to be taken into account. Therefore, mathematical modelling to determine the OPS will change accordingly. Furthermore, when cognitive radio features are incorporated into the MIMO based sensor network architecture, it would make the mathematical analysis non-trivial. Moreover, the previous work that propose a conventional MIMO based WSNs do not consider the additional interference caused by the surrounding users sharing the same band. This motivated us to introduce the paradigm of cognitive radio along with conventional MIMO-WSNs where the nodes along with MIMO and an optimal packet size mode of transmission would also have the additional feature of cognitive channel sensing and switching based on the network conditions. This helps to counter the effects from the non-cognitive users. Moreover, in our previous works [11], we have established performance improvement for cognitive radio assisted point-to-point WSNs with OPS in terms of overall energy consumption and other key networking metrics. This lead us to the envisage the concept of MIMO assisted cognitive radio enabled wireless sensor networks with optimal packet size (MIMO-CRSN-OPS) which has to best of our knowledge has not been explored so far within the current state of the art.Rigorous analysis through our simulations demonstrate performance improvement of our system as compared to general point to point CRSN architecture.

The main contribution of our paper could be summarized as follows.

1) Firstly, we formulated a joint optimization problem to determine the optimal packet size for a MIMO-Cognitive radio based sensor networks architecture which has not been done so far.
2) Secondly we propose two algorithms to solve the proposed optimization problem. First algorithm is based on Exhaustive Search and the second low complexity suboptimal algorithm is based on solving the conventional Karush-Kuhn-Tucker conditions.
3) Thirdly the MIMO-CRSN framework with optimal packet size mode of transmission is incorporated with a distributed time slotted channel access scheme and a CSMA/CA assisted centralized common control channel based channel access scheme.

This paper is organized as follows. Section II highlights the related work. Section III describes the system model. Section IV describes the different transmission states involved

during cognitive mode of transmission and estimation of the involved channel sensing time for a given detection and false alarm threshold. Section V shows the modelling of the basic optimization problem used to determine the OPS for CRSN. Section VI describes the remodelling and simplification of the optimization problem with variable rate m-QAM based modulation scheme. Section VII describes the proposed algorithm based on exhaustive search and Newton-Raphson assisted KKT-based approach. Numerical results are demonstrated in Section VIII and Section IX concludes the paper.

II. RELATED WORKS

Among the notable works in this area, the authors of [16] presented an exhaustive survey paper on the cognitive radio sensor networks with special emphasis on resource allocation to guarantee quality of service. The concept of Energy Harvesting Cognitive Radio Sensor Networks (EHCRSNs) is proposed by the authors of [17]. In this paper the authors have developed an aggregate network utility optimization framework to design a resource management algorithm based on Lyapunov optimization. In [18] the authors have extended the concept of cognitive radio to propose a cooperative wireless energy harvesting and spectrum sharing for the emerging 5G mobile standards where the secondary users relays and harvest energy from the primary user simultaneously. The authors of [19] have proposed a novel paradigm of heterogeneous cognitive sensor network where two separate categories of sensor nodes are considered within a given network. There are dedicated spectrum sensors which continuously monitor the channel availability and data sensors which scans the area of interest and transmit relevant data from the area of interest. A spectrum scheduling algorithms exclusively for the spectrum nodes and resource allocation algorithm for the data nodes jointly enhances the performance of the overall system. In [20] the authors based on queueing theory and classical KKT optimization technique devised an efficient relaying mechanism for a cognitive radio sensor networks architecture where the secondary users maintain a separate queue to relay the data packet of the primary users taking into account the secondary delay, power consumption and admission control acceptance factor. In [21] the authors have proposed a novel cognitive adaptive medium access control scheme (CAMAC) which adapts its channel sensing time and duty cycle to make the system more power efficient. In [22] a spectrum aware cluster based routing protocol is proposed by the authors for multimedia routing. A novel dynamic channel access strategy is proposed in [23] for a clustered CRSN architecture which improves the energy efficiency and throughput both for the intracluster and intercluster communication. It also takes into due consideration appropriate cluster head selection based on available energy and spectrum availability. The authors in [24] proposed a cognitive communication assisted cross layer approach for the smart grid applications. The challenges associated with the harsh smart grid environment and the differential traffic flow are addressed by formulating the problem to as a Lyapunov drift optimization. In [25] the classical challenge of spectrum sensing data falsification during joint channel sensing is addressed. An energy efficient collaborative spectrum sensing technique is proposed which considers both independent and collective false spectrum data reporting as a probabilistic measure. Authors of [26], [27], [28] and [29] addresses various challenges associated with the cooperative spectrum sensing and selection of the best nodes within a cluster to improve the detection reliability. In [30] a joint channel access and sampling rate control strategy for energy harvesting CRSNs is proposed. A joint optimization problem based on mix-integer non-linear programming (MINLP) is formulated with fluctuating energy harvesting parameter which maximizes the network utility metric by adapting sampling rate and channel access with energy consumption, capacity and interference as constraints. Among the initial works in the area of packet size optimization for MIMO based systems, the authors of [15] proposed an energy efficient MIMO communication system with packet length adaption with congestion control and delay constraint. M/G/1 queuing theory is used to model the congestion control and delay parameters. A novel event zone to sink aware clustering protocol is proposed by the authors of [31]. The clustering is assumed to be accomplished in two phases which includes determination of the eligible nodes within the event to sink corridor and second phase is the cluster formation. Based on this approach the average re-clustering probability and expected coverage area is determined in this work. In [32], the authors proposed an utility based spectrum access for CRSNs based on random access control. The formulated non-convex optimization problem was solved by the proposed primal decomposition based iterative algorithm. In order to select the best nodes to increasing the channel sensing accuracy in case of joint spectrum sensing , the authors of [4] modelled the mathematical formulation as a binary knapsack problem and solved using dynamic programming taking into account major system constraints like energy consumption and network lifetime. A scalable routing protocol for the CRSNs exclusively for an indoor environment with suitable channel model is proposed in [33]. The simulation results are validated by the results obtained from real time indoor deployment of the sensor nodes. Authors of [34] addressed the issue of optimal spectrum assignment in CRSNs under various network constraints. The modelled MINLP was transformed to a binary linear programming (BLP) using various constraint relaxation techniques. The problem was modelled as mixed integer programming problem. In [35] the authors proposed to improve the spectral efficiency of the CRSNs using in network computation which would minimise the required transmissions and facilitate more simultaneous transmission. A greedy networking algorithm is proposed to improve the quality of service.

III. SYSTEM MODEL

Fig. 1 shows the basic system model of the proposed MIMO-CRSN framework. The network consists of a large number of sensor nodes. Few of the nodes are equipped with cognitive channel sensing and switching feature all of which are operating in the ISM 2.4 GHz band. In addition there are other services like WiFi, Bluetooth, Zigbee and unlicensed

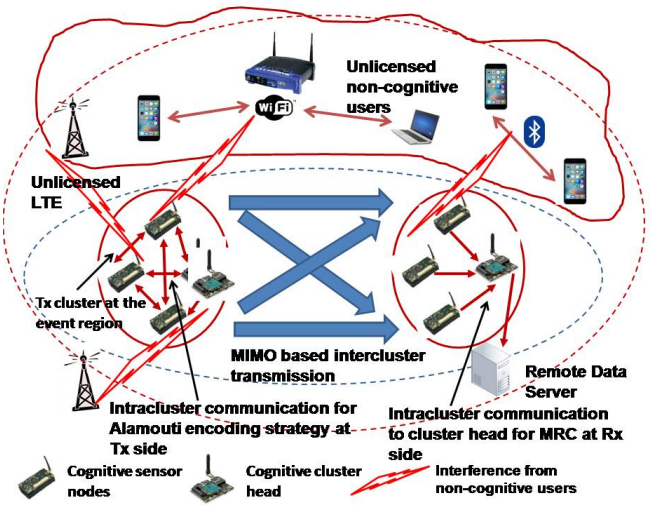

Fig. 1. Basic system architecture of delay sensitive cognitive radio wireless sensor network

LTE which are also operating in the same unlicensed frequency band causing interference to the cognitive users. These services along with other sensor nodes dedicated for other applications without cognitive feature are collectively termed as non-cognitive users. Whenever an event is triggered, few of the cognitive nodes within the region of event senses the physical phenomenon and transmit the sensed data either through multihop or directly to a distant data gathering server. In order to facilitate (2×1) Alamouti MIMO encoding the cognitive sensor nodes within the event region forms a cluster. In Fig. 1, there are 4 cognitive nodes in a single cluster. This value is denoted as M_t. Among the cognitive nodes in a cluster, there can be a cluster head which is responsible for some additional functionalities like data aggregation or decision fusion in case of cooperative channel sensing. These cognitive nodes initially carries out local information exchange to enable Alamouti encoding. Once the intracluster phase is over, these cognitive nods do form a virtual antenna array and transmit its data for the long haul communication. In case of a multihop network the data is transmitted either to another intermediate cluster which is not in the event region but do assist to relay the information from the cluster it the event region. In this case there has to be local information exchange at the receiver cluster as well as the Alamouti encoded orthogonal symbols must combined using standard techniques like maximum ratio combining and subsequently decoded to retrieve the originally transmitted symbols. Upon decoding, the retrieved symbols can re-encoded and transmitted to the next available cluster closer to the sink or to the sink directly depending on the network topology. In our analysis for the sake of simplicity we are assuming a single hop system where the the information from the cluster in the event region is transmitted to the sink or gateway equipped with a single antenna. It is also assumed that the mean average intracluster distance among the cognitive nodes (d_{loc}) is much lesser than the long haul distance.

The cognitive nodes are aware of apriori information like the mean busy time (l_p) and the average idle time (v_p) of the non-cognitive users. The non-cognitive traffic is assumed to be be exponentially distributed. Based on these two parameters, the average probability of occupancy Pr_{on} and Pr_{off} are calculated. These two parameters are estimated to be as $Pr_{on} = \frac{l_p}{(l_p+v_p)}$ and $Pr_{off} = 1 - Pr_{on}$. Depending on these two critical parameters and other network conditions, the cognitive nodes would adapt its various parameters like packet size, modulation level (bits/symbol) and transmit power to improve the performance of the system [9]. It is assumed there are C data channels accessed simultaneously by both cognitive and non-cognitive users. If there are M cognitive users in the region of event, effectively $\left(\frac{M}{M_t}\right)$ number of clusters are in contention to share the C data channels along with the non-cognitive users are each cluster selects the same channel for data transmission in the proposed MIMO-CRSN system. Moreover, it is assumed that the channel state information (CSI) and noise characteristics are known both to the transmitter and receiver in this paper. The information from the cognitive nodes within the region of event must reach the destination within τ_d seconds. Furthermore, the duration of interference caused by these cognitive users to the other surrounding services must be lesser than a certain percentage of the average busy time of the non-cognitive users denoted as I_{max}. In a single cluster only one of the member cognitive nodes senses the channel because it is assumed that the average intracluster distance among the nodes is small as compared to the long haul intercluster or cluster to sink distance.

IV. *Cognitive radio based transmission states*

Energy based channel detection scheme is considered for the proposed MIMO-CRSN framework in this paper. The are well established literatures available in this area [36], [37] and [38] which presents a comprehensive mathematical analysis and formulation to estimate various key parameters like the probability of detection P_d, false alarm P_f and misdetection P_{md}. Probability of detection gives us a measure of how accurately the signals from the primary users or non-cognitive users in our system could be detected correctly by the cognitive users. Misdetection corresponds to the wrong detection of the non-cognitive users whereas false alarm is the measure of wrong detection of the presence of non-cognitive users which leads to a missed opportunity of transmission by the cognitive users. As elaborately explained in our previous work [11] and [9], the respective probabilities of being in these states would be

$$Pr_1 = Pr_{on}P_d \tag{1}$$

$$Pr_2 = Pr_{on}(1 - P_d) \tag{2}$$

$$Pr_3 = Pr_{off}P_f, \tag{3}$$

where Pr_1, Pr_2 and Pr_3 are the respective probabilities of being into the states of detection, misdetection and false alarm. Furthermore, into account the cognitive transmission aspect in case of a distributed channel access scheme, more than a single cognitive user could select the same data channel concurrently

which might lead to co-user interference. The probability of such an event occurring is estimated to be as

$$Pr_4 = Pr_{off}(1-P_f)\left[1-\left\{\frac{(CPr_{off}-1)}{CPr_{off}}\right\}^{M-1}\right], \quad (4)$$

where M is the number of contending users in the system and $\left\{\frac{(CPr_{off}-1)}{CPr_{off}}\right\}^{M-1}$ is the probability of more than two users not selecting the same channel. Ergodic behaviour of all the non-cognitive over the C data channels leads to effective CPr_{off} available data channels. In addition there can be a possibility that the cognitive users finds a channel to be vacant and during the transmission duration the non-cognitive user starts transmitting over the same data channel leading to collision and packet drop. The probability of such an event occurring denoted as Pr_5 would be

$$Pr_5 = (Pr_{off}(1-P_f) - Pr_4)Pr(V_p \leq \frac{l_s}{R}) \quad (5)$$
$$Pr_5 = (Pr_{off}(1-P_f) - Pr_4)\int_{\frac{l_s}{R}}^{\infty} \frac{1}{v_p} e^{\frac{-t}{v_p}} dt$$
$$Pr_5 = (Pr_{off}(1-P_f) - Pr_4)\left(1 - e^{\frac{-l_s}{Rv_p}}\right)$$

where, v_p is the average idle time, R is the data rate, l_s is the packet size in bits, P_{off} is the probability of unoccupancy by the non-cognitive users, P_f is the false alarm. This state is feasible if and only if the state of co-users interference (Pr_4) as estimated in (4) doesn't occur. Finally the state of successful transmission is achieved when both state of co-user interference and collision doesn't occur and the idle time of the non-cognitive users is greater than the packet transmission duration which results into

$$Pr_6 = e^{\frac{-l_s}{Rv_p}}(Pr_{off}(1-P_f) - Pr_4). \quad (6)$$

In addition, during the state of Misdetection the interference to the non-cognitive users could last for entire duration of the cognitive transmission or the cognitive users could decide to vacate the channel during the transmit duration of the cognitive users. The probability of such an event occur would be $Pr(L_p \leq \frac{l_s}{R}) = (1 - e^{\frac{-l_s}{Rl_p}})$. Since such event also must be accompanied by the unoccupancy of the non-cognitive users therefore, the probability of being into such state would be $Pr_{off}(1 - e^{\frac{-l_s}{Rl_p}})$. Similarly the probability of such event not occurring during the state of misdetection or in other words the non-cognitive user's transmission lasting throughout the duration of the cognitive packet transmission would be $1 - Pr_{off}(1 - e^{\frac{-l_s}{Rl_p}})$. Since $Pr_{on} + Pr_{off} = 1$ thus, the probability that there will be collision and packet drop for cognitive users during the state of collision would be $\left(Pr_{on} + Pr_{off}e^{\frac{-l_s}{Rl_p}}\right)$

As shown by the authors of [37], depending on the gaussian probability distribution function of the received interference power from the non-cognitive users and the central limit theorem, the probability of detection (P_d) and false alarm (P_f) is estimated to be as

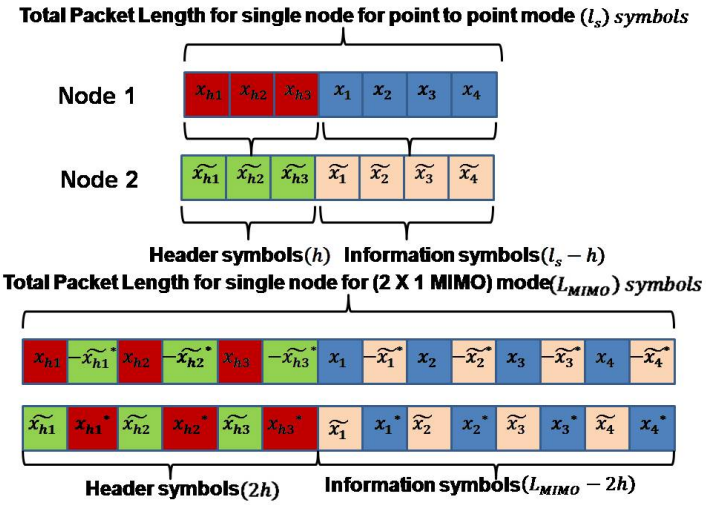

Fig. 2. Basic system architecture of delay sensitive cognitive radio wireless sensor network

$$P_d = Q\left(\left(\frac{\lambda}{\sigma_u^2} - \gamma_{pr} - 1\right)\sqrt{\frac{\tau_s f_s}{2\gamma_{pr}+1}}\right) \quad (7)$$
$$P_f = Q\left(\left(\frac{\lambda}{\sigma_u^2} - 1\right)\sqrt{\tau_s f_s}\right), \quad (8)$$

where τ_s is the channel sensing duration, γ_p is the received signal strength at the cognitive transmitter from the non-cognitive users, λ is the detection threshold of the energy based detector and σ_u^2 is the total noise power. Taking λ as an implicit variable the sensing time required for a specific P_d and P_f threshold for a specific γ_{pr} turns out to be

$$\tau_s = \frac{1}{2B\gamma_{pr}^2}\left[Q^{-1}(P_f) - Q^{-1}(P_d)\sqrt{2\gamma_{pr}+1}\right]^2. \quad (9)$$

In the remaining part of this paper γ_p is denoted as SNR_{pr} and $\sigma_u^2 = N_0 B$ where N_0 is the noise power spectral density whose value is -171 dBm/Hz and B is the channel bandwidth at 1 MHz.

V. Problem Formulation for MIMO-CRSN Architecture

A. Formulation and analysis of the cost function

Determination of optimal packet size in MIMO-CRSN architecture involves formulation of a cost function which takes into account the overall energy efficiency $(e_{\mathbf{mimo}})$ and the packet reliability $(r_{\mathbf{mimo}})$ of the system. It is dependent on the packet size $l_s^{\mathbf{MIMO}}$ symbols. Furthermore, for MIMO based architecture the additional overhead energy consumed during the intracluster phase at the transmitter end to form the virtual MIMO antenna array denoted as $E_{local}^{T_x}$ in order to facilitate Alamouti encoding plays a significant role that needs to be considered. Moreover, factors contributed by the cognitive functionalities such as channel sensing, channel handoff, channel decision alongside energy consumed during

transient phases like activation from sleep to wake up mode must also be included. Based on these collective factors an appropriately designed cost function could provide an optimal packet size for MIMO-CRSN architecture.

For MIMO-CRSN architecture the data packets from a given number multiple nodes in a single cluster participating in data communication (M_t) must transmit its data simultaneously and in a synchronized manner to the sink node for proper decoding of the orthogonally encoded Alamouti bit streams from M_t sensor nodes. Therefore, unlike point-to-point CRSN architecture where a single data packet from its corresponding sensor node is used to estimate the OPS, in MIMO CRSN mode data packets from M_t must be considered jointly and to be treated as a single data superpacket denoted as $l_s^{\mathbf{MIMO}}$. In Fig. 3, an Alamouti encoded (2×1) MIMO-CRSN packet structure is described. For example, for two sensor nodes $(M_t = 2)$ sensor nodes in a given cluster, it is assumed that each node has four independent data symbols x_i and $\tilde{x_i}$ for node 1 and 2 respectively where $i = \{1, 2, 3, 4\}$ and three independent header symbols x_{hj} and $\tilde{x_{hj}}$ where $j = \{1, 2, 3\}$ that is to be transmitted to the sink node. Header segment of a data packet contains critical information like the node id and additional bits for other features like channel estimation, cyclic redundancy check etc. Assuming both the independent header and data symbols from the two nodes must reach the destination and decoded correctly, for Alamouti encoded system, in first time slot node 1 and 2 will have to transmit x_i and $\tilde{x_i}$ while in second time slot node 1 and 2 needs to transmit $-\tilde{x_i}^*$ and x_i^* respectively. Same holds true even for the header symbols. Therefore, as shown in Fig. 3, the MIMO data packet from each of the sensor node is likely to have 14 Alamouti encoded data symbols, 6 of which attributed by the encoded header symbols and remaining 8 encoded data symbols. Both node 1 and 2 will have to transmit these 14 orthogonally encoded symbols simultaneously in a synchronized manner for proper detection at the sink. The sink could be the final gateway itself in case of a single hop scenario or it could be the cluster head of an intermediate cluster. Therefore, in our example the packet size for each node operating under MIMO mode $l_s^{\mathbf{MIMO}}$= 14 symbols. Our objective is therefore to obtain the optimal size of $l_s^{\mathbf{MIMO}}$ denoted from now on as $l_{opt}^{\mathbf{MIMO}}$ which is the optimal packet size for our proposed MIMO-CRSN architecture.

For the proposed MIMO-CRSN architecture, to simplify our further analysis we assume the long haul transmission energy consumption per independent symbol to attain a specific bit error rate threshold denoted as $k_{sym1}^{\mathbf{MIMO}}$ as shown by the authors in [12]. It is however important to mention that although $(14 + 14)$= 28 Alamouti encoded symbols are transmitted 14 symbols each from node 1 and 2 respectively, the overall energy consumption for the transmission of the MIMO superpacket generated by M_t= 2 participating nodes in the cluster will be $k_{sym1}^{\mathbf{MIMO}} \times 14$ and not 28. This is due to the fact that when we consider energy consumption for the independent symbols, while using full rate code like (2×1) Alamouti code the effect of transmitting the conjugate symbols x_i^* and $-\tilde{x_i}^*$ in the even time slots is already included in the $k_{sym1}^{\mathbf{MIMO}}$. Since in the MIMO superpacket there are 14 independent symbols generated 7 (3 header symbols + 4 data symbols) each from node 1 and node 2, the overall transmission energy consumption turns out to be $(k_{sym1}^{\mathbf{MIMO}} \times 14)$. For variable rate m-QAM modulation scheme the energy consumption per bit $k_1^{\mathbf{MIMO}}$ could be obtained just by normalizing $(k_{sym1}^{\mathbf{MIMO}})$ by b where b is the modulation level (bits/symbol).

For notational convenience $l_s^{\mathbf{MIMO}}$, $l_{opt}^{\mathbf{MIMO}}$ and $k_1^{\mathbf{MIMO}}$ are denoted as l_s, l_{opt} and k_1 for the remaining sections in this paper. Both $l_s^{\mathbf{MIMO}}$ and $l_{opt}^{\mathbf{MIMO}}$ are in bits. Based on the above premise, the cost function $(\eta^{\mathbf{mimo}})$ to determine the optimal packet size based on energy efficiency and reliability metric for the proposed MIMO-CRSN architecture is mathematically formulated to be as

$$\eta_{\mathbf{mimo}}(l_s) : e_{\mathbf{mimo}}(l_s) \times r_{\mathbf{mimo}}(l_s) \tag{10}$$

It is assumed that in general for each sensor node the header (h) typically contains 6 bytes or 48 bits as per IEEE 802.15.4 protocol. If this value obtained as per standard is assumed to be fixed, data packet from each of the nodes within the MIMO superpacket with length l_s would contain total $(l_s - M_t h)$ independent data bits contributed by M_t users within the cluster. In order to form the virtual MIMO cluster to enable Alamouti encoding at the transmitter end, there has to be intracluster information exchange. It is assumed that k_{loc} is the energy consumption per bit for the local information exchange. Therefore, the total energy consumption for intracluster information exchange at the transmitter end $(E_{local}^{T_x})$ would be

$$E_{local}^{T_x} = k_{loc}(l_s - M_t h). \tag{11}$$

Therefore,

$$e_{\mathbf{mimo}}(l_s) = \frac{k_1(l_s - M_t h)}{k_1 l_s + E_{local}^{T_x} + E_{tot}}, \tag{12}$$

where k_1 is the energy consumption per bit required for long haul communication, l_s is the packet size and

$$E_{tot} = E_{hf} + E_{sens} + E_{dec} + E_{add}, \tag{13}$$

where E_{sens} is the channel sensing energy , E_{hf} is the energy consumed for channel handoff, E_{dec} is the energy consumed to reach a decision about a channel and E_{add} is the additional energy consumption involved because of the spectrum decision, handoff and other transient power consumption with the transceiver.

$$E_{sens} = \tau_s \times P_{sens}, \tag{14}$$

where τ_s is the channel sensing time which is dependant on received non-cognitive SNR (γ_{pr}) obtained from (14) and P_{sens} is power consumption due to channel sensing nearly equal to 110 mW [30].

Energy consumed for channel switching will depend on the condition that the existing channel is sensed as busy and any one of the other $(C - 1)$ available channels is unoccupied by the non-cognitive users. Therefore, it is calculated to be as

$$Pr_{idle} = Pr_{off}(1 - P_f) + Pr_{on}(1 - P_d) \tag{15}$$

$$Pr_{busy} = (Pr_{off}P_f + Pr_{on}P_d)^{(C-1)} \tag{16}$$

$$Pr_{sw} = (1 - Pr_{idle})(1 - P_{busy}). \tag{17}$$

As per authors of [40], energy consumed for channel switching (E_{hf}) in practical applications for a relaxed scenario when the channel center frequencies are close by is around 2 mJ. Therefore average energy consumed for channel handoff for CR architecture turns out to be $Pr_{sw}E_{hf}$.

In MIMO-CRSN architecture the data packets from M_t nodes within the cluster must be transmitted and received in a simultaneous and synchronized manner. It is assumed that drop of data packet from any single M_t user within the cluster would lead to failed detection of the entire MIMO superframe. Therefore, for correct detection the packets from each of the M_t users must reach and detected correctly at the receiver. For each node, the packet error rate $(PER_{\mathbf{single}})$ and reliability $(r_{\mathbf{single}})$ is calculated to be as

$$PER_{\mathbf{single}} = 1 - (1 - \overline{P_e})^{l_s} \tag{18}$$

$$r_{\mathbf{single}} = 1 - PER_{\mathbf{single}}, \tag{19}$$

where $\overline{P_e}$ is the average bit error rate of the MIMO-CRSN model and l_s is the packet size.

Therefore, the overall reliability of the MIMO superpacket is estimated to be as

$$r_{\mathbf{mimo}}(l_s) = r_{\mathbf{single}}^{M_t} \tag{20}$$

$$r_{\mathbf{mimo}}(l_s) = (1 - PER_{\mathbf{single}})^{M_t} = (1 - \overline{P_e})^{M_t l_s}. \tag{21}$$

Therefore, the cost function is simplified to

$$\eta_{\mathbf{mimo}}(l_s) = \frac{k_1(l_s - M_t h)}{k_1 l_s + k_{loc}(l_s - M_t h) + E_{tot}}(1 - \overline{P_e})^{M_t l_s}. \tag{22}$$

The motivation to consider the cost function as a multiplicative factor of the energy-efficiency $e_{\mathbf{mimo}}$ and reliability $r_{\mathbf{mimo}}$ is owes to fact that the formulated cost function in this case will be concave with respect to the packet length l_s with an unique global maxima. Other modes of designing the same like weighted-sum approach would not guarantee a concave behaviour of the cost function which is needed to find the optimal packet size both mathematically and intuitively. Analyzing the cost function further, the first and the second derivative of the cost function yields

$$\eta_{\mathbf{mimo}}(l_s)^{'} = Z_1(l_s)Z_2(l_s), \tag{23}$$

where $Z_1(l_s)$ and $Z_2(l_s)$ are dummy variables evaluated to be as

$$Z_1(l_s) = \frac{E_{tot}k_1 + k_1^2 M_t h}{(k_1 + k_{loc})l_s + E_{tot} - k_{loc}M_t h} + k_1(l_s - M_t h)M_t \ln(1 - \overline{P_e}) \tag{24}$$

$$Z_2(l_s) = \frac{(1 - \overline{P_e})^{M_t l_s}}{(k_1 + k_{loc})l_s + E_{tot} - k_{loc}M_t h}. \tag{25}$$

By replacing $E_{tot} - k_{loc}M_t h = Z_3$, the double derivative of the cost function turns out to be

$$\eta_{\mathbf{mimo}}(l_s)^{''} = Z_1(l_s)^{'} Z_2(l_s) + Z_2(l_s)^{'} Z_1(l_s). \tag{26}$$

The double derivative of the dummy variables $Z_1(l_s)$ and $Z_2(l_s)$ are calculated to be as

$$Z_1(l_s)^{'} = \ln(1 - \overline{P_e})M_t k_1 - \frac{(E_{tot}k_1 + k_1^2 M_t h)(k_1 + k_{loc})}{\{(k_1 + k_{loc})l_s + Z_3\}^2} \tag{27}$$

$$Z_2(l_s)^{'} = \frac{Z_4(l_s)}{\{(k_1 + k_{loc})l_s + Z_3\}^2}, \tag{28}$$

where

$$Z_4(l_s) = \{(k_1 + k_{loc})l_s + Z_3\}\ln(1 - \overline{P_e})M_t(1 - \overline{P_e})^{M_t l_s} (k_1 + k_{loc})(1 - \overline{P_e})^{M_t l_s}. \tag{29}$$

Considering the fact that $\overline{P_e} \ll 1$, it implies $\ln(1 - \overline{P_e}) \approx 0$. Using (27), (28) and (29) it can be proven that $\eta_{\mathbf{mimo}}^{''}(l_s) < 0$. Therefore, the cost function $\eta(l_s)$ is a concave function with respect to the packet size l_s with an unique maxima. Therefore, the optimal packet size turns out to be l_s^* which maximizes the following cost function as long as all the posed constraints criteria are satisfied.

$$\underset{l_s}{\boldsymbol{max}}\, \eta_{\mathbf{mimo}}(l_s) = \frac{k_1(l_s - M_t h)}{(k_1 + k_{loc})l_s + E_{tot} - k_{loc}M_t h}(1 - \overline{P_e})^{M_t l_s}. \tag{30}$$

For a fixed average BER $\overline{P_e}$, packet size (l_s) and E_{tot}, differentiating the cost function $\eta_{\mathbf{mimo}}$ with respect to k_1 leads to

$$\frac{\partial \eta_{\mathbf{mimo}}}{\partial k_1} = \frac{k_{loc}(l_s - M_t h)l_s + Z_3(l_s - M_t h)}{\{k_1 + k_{loc})l_s + Z_3\}^2}(1 - \overline{P_e})^{M_t h} \tag{31}$$

As $l_s > M_t h$, from the basic assumption, it can be proven that the cost function $\eta_{\mathbf{mimo}}$ is an increasing function of k_1 for fixed value of l_s, $\overline{P_e}$ and other parameters remaining constant.

The energy consumption per bit k_1 depends upon the power consumed by the power amplifiers and the circuit components of the transceiver nodes [13]. In case if m-QAM modulation scheme is used, this energy consumption per bit will depend on the modulation level (b) as the data rate (R) will depend on b for a fixed symbol rate for the system (R_s) .

$$k_1 = (P_{PA} + P_c)\frac{1}{bR_s}. \tag{32}$$

Energy consumption per bit k_1 is a function of the modulation level b. It has been extensively discussed in our previous work and previous established literatures that in case of variable rate modulation scheme, for relatively smaller distances and for given fixed BER threshold, the energy consumption per bit k_1 will exhibit a convex behaviour with respect to the modulation level b. This behaviour holds true both for point to point and MIMO systems alike. The rationale behind such behaviour is contributed by the fact that increase in the modulation level increases the data rate since $R = bR_s$ and minimizes the transmit duration. Upto a specific value of b say

b^* the transmit duration will be dominant factor therefore, the value of k_1 would decrease. However, the power consumption of the power amplifier P_{PA} is an increasing function with respect to b. Beyond the value of b^*, P_{PA} will become the dominant factor instead of the transmit duration thus resulting into an increased value of k_1.

In the subsequent section it will be shown that the average BER $\overline{P_e}$ of the proposed MIMO-CRSN architecture will depend on the probabilities of being in the state of misdetection and collision. Under these cases the data packet from the cognitive experience interference either from the non-cognitive users or from other cognitive users selecting the same channel. The probabilities of these states directly depends upon the transmit duration of the data packet or in other words the packet length (l_s) as shown in Section IV. Therefore, the energy consumption per bit k_1 to attain a specific BER threshold will be dependant on the packet size along with the modulation level thus making it $k_1(l_s, b)$, a function of both l_s and b. It is already shown from (26) to (29) , the cost function $\eta_{\mathbf{mimo}}(l_s)$ will be concave function of the packet size l_s for a fixed $\overline{P_e}$, fixed modulation level b and its corresponding energy consumption per bit $k_1(b)$. However, in our case since k_1 is also dependant on l_s makes further analysis non trivial. Furthermore, it is observed that for fixed modulation level b, the concavity of the cost function $\eta_{\mathbf{mimo}}(l_s, b)$ will be preserved even though $k_1(l_s, b)$ now being dependant on the packet size. It is also observed that $k_1(l_s)$ will be an increasing function of l_s for fixed value of b. However, the magnitude of increase in the k_1 value with increasing l_s for a fixed b is much smaller to affect the very nature of the cost function η. It is proven $\eta_{\mathbf{mimo}}(l_s)^{''} < 0$ in our appendix section. Based on this argument for a given modulation level b, the optimal packet size l_s^* which maximizes the cost function could be written as

$$\overline{l_s^*} = \left\{ \underset{l_s}{max}\, \eta_{\mathbf{mimo}}(l_s, b) \right\} \forall b, \tag{33}$$

where $\overline{l_s^*}$ is the set of optimal packet size for different modulation levels. Along finding the optimal packet size for the MIMO-CRSN architecture, it is also our objective to ensure the system must consume minimum energy which is one of the essential requisite for any sensor network architecture. This essentially leads us to the conclusion that the selection of the appropriate modulation level b holds the key for which the the energy consumption per bit $k_1(b)$ would be minimum. From (31) it is proven that the cost function $\eta_{\mathbf{mimo}}$ will be an increasing function of k_1 when packet length and BER threshold is fixed. Moreover, the authors of [13] has shown that k_1 will show a convex behaviour with respect to b for a fixed $\overline{P_e}$. Therefore, the optimal modulation level b^* must be selected among the set of given modulation levels for which the energy consumption per bit k_1 will be minimum. Based on this and the previous property it can be easily concluded that the cost function $\eta_{\mathbf{mimo}}$ too will exhibit a convex behaviour with respect to modulation level b. For individual modulation levels, its corresponding optimal packet size is already estimated in (33) as $\overline{l_s^*}$

$$\overline{b^*} = \left\{ \underset{b}{min}\, \eta_{\mathbf{mimo}}(l_s^*, b) \right\} \forall\, b. \tag{34}$$

Therefore,combining (33) and (34), the cost function to obtain the optimal packet size and optimal modulation level could be written as a min-max problem

$$\underset{b}{\boldsymbol{min}} \left\{ \underset{l_s}{\boldsymbol{max}}\ \eta_{\mathbf{mimo}}(l_s,\, b) \,=\, \frac{\boldsymbol{k_1(l_s,b)}(l_s - M_t h)(1-\overline{P_e})^{M_t l_s}}{(\boldsymbol{k_1(l_s,b)} + k_{loc}) l_s + Z_3} \right\}, \tag{35}$$

where $Z_3 = E_{tot} - k_{loc} M_t h$.

B. Modelling of the total interference time constraint for the non-cognitive user

The duration for which the non-cognitive users experiences interference from the cognitive secondary users plays an important role for any cognitive radio based network. As explained in [11], [9], it depends upon the probabilities of being into the state of misdetection and collision. However, in case of MIMO-CRSN architecture the number of nodes in a given cluster (M_t) will transmit its data sharing the same channel. Therefore, if there are M total number of users participates in data transmission over C data channels, there will be effectively $\frac{M}{M_t}$ number of users among which there will be contention within C data channels. Therefore, the probability of co-user selection Pr_4 for MIMO-CRSN architecture will now turn out to be

$$Pr_4^{\mathbf{mimo}} = Pr_{off}(1 - P_f) \left\{ 1 - \left(\frac{CPr_{off} - 1}{CPr_{off}} \right)^{\left(\frac{M}{M_t} - 1\right)} \right\}. \tag{36}$$

Based on $Pr_4^{\mathbf{mimo}}$, the probability of collision will be

$$Pr_5^{\mathbf{mimo}} = \left\{ Pr_{off}(1 - P_f) - Pr_4^{\mathbf{mimo}} \right\} e^{\frac{-l_s}{Rv_p}} \tag{37}$$

As explained in [9] and [11], during the state of misdetection the duration of interference with the non-cognitive users could last either for the entire duration of the packet transmission of the cognitive user or the non-cognitive user may decide to vacate the channel during the transmission phase of the cognitive user. In the later case the non-cognitive users will not experience any interference from the cognitive users. Based on above, the total average duration of interference cause to the non-cognitive users for the proposed MIMO-CRSN architecture boils down to

$$\tau_{inf}^{\mathbf{mimo}}(l_s, b, P_d, P_f, M_t) = \frac{l_s}{R} \frac{Pr_2 \left(Pr_{on} + Pr_{off} e^{\frac{-l_s}{Rl_p}} \right) + Pr_{on} Pr_5^{\mathbf{mimo}}}{Pr_2 + Pr_5^{\mathbf{mimo}}}, \tag{38}$$

where $R = bR_s$ is the data rate of the system.

Therefore, the ratio of the average interference time to the average busy transmission time of the non-cognitive user denoted by I_{nc} will be,

$$I_{nc}^{\mathbf{mimo}}(l_s, b, P_d, P_f, M_t) = \frac{\tau_{inf}^{\mathbf{mimo}}}{l_p}. \tag{39}$$

$I_{nc}^{\mathbf{mimo}}$ must be lesser than I_{max} which is application specific constraint threshold. Therefore, from (38) and (39) the constraint could be written as

$$c_1^{\mathbf{mimo}}(l_s, b, P_d, P_f, M_t) = I_{nc}^{\mathbf{mimo}}(l_s, b, P_d, P_f, M_t) - I_{max} \leq 0 \tag{40}$$

C. Modelling of the end to end delay constraint for the cognitive user

An infinite Stop and Wait ARQ scheme for the proposed MIMO-CRSN architecture is considered which is used to calculate the average time to transmit each data packet and takes into account the retransmission overheads [9], [11]. For M cognitive users participating in data communication each of which has K bits to transmit, there are M_t sensor nodes in each cluster. Therefore, there are $\frac{M}{M_t}$ number of clusters in the MIMO-CRSN network. For each of these clusters, there has to be local intracluster information exchange to enable Alamouti MIMO encoding. This consumes overhead delay. Furthermore, due to the cognitive feature of the network just like point-to-point CRSN architecture there will be additional delay incurred due to channel sensing, channel decision, handoffs, processing delay at each hop for each packet and transient delay due to wake up and sleep functionalities of the sensor nodes.

The average packet error rate for the for the MIMO-CRSN model could be directly obtained from (21) as

$$PER^{\mathbf{mimo}}(l_s) = 1 - r_{\mathbf{mimo}}(l_s). \tag{41}$$

Based on the Stop and Wait ARQ retransmission mechanism the average delay for the long haul transmission will be

$$E(T) = T_s \left(1 + \frac{PER^{\mathbf{mimo}}}{1 - PER^{\mathbf{mimo}}}\right) \tag{42}$$

$$E(T) = T_s \left(1 + \frac{1 - \left(1 - \overline{P_e}\right)^{M_t l_s}}{\left(1 - \overline{P_e}\right)^{M_t l_s}}\right),$$

where $T_s = \left(\frac{l_s}{R} + \tau_{add}\right)$ where $\frac{l_s}{R}$ is the data transmission time.

$$\tau_{add} = \tau_d + \tau_s + \tau_{dec} + \tau_{hf} + \tau_{sl/wk} \tag{43}$$

is the additional delay caused due to processing at each hop (τ_d), channel sensing time (τ_s), handoff (τ_{hf}), spectrum decision (τ_{dec}), and transient time for the receiver to wake up from sleep to active model. Values of τ_{hf} and τ_{dec}.

$$\tau_{total}^{\mathbf{mimo}} = \frac{MK\overline{n}}{(l_s - M_t h)} \left\{(1 + M_t\overline{P_e} l_s)\left(\tau_{total} + \frac{l_s}{R}\right) + \frac{(l_s - M_t h)}{R_{loc}}\right\}, \tag{44}$$

where $R_{local} = b_{loc}R_s$ is the data rate of the system during intracluster communication, b_{loc} is the corresponding modulation level, $\overline{n}$ is the average number of hops and $k = \frac{\tau_d}{MK\overline{n}}$ where τ_d is the total end to end delay threshold. For much shorter distances for intracluster communication, the modulation level is usually high [12].

The total delay $\tau_{total}^{\mathbf{mimo}}$ must be less than or equal to a specific end to end delay threshold τ_d. Therefore, (44) could be rewritten as

$$c_2^{\mathbf{mimo}}(l_s) = \tau_{total}^{\mathbf{mimo}} - \tau_d \leq 0 \tag{45}$$

$$c_2^{\mathbf{mimo}}(l_s) = \frac{M_t\overline{P_e}}{b} l_s^2 + \left(\frac{1}{b} + \frac{1}{b_{loc}} + M_t\overline{P_e}\tau_{tot}R_s - kR_s\right) + \left(M_t hkR_s + \tau_{tot}R_s - \frac{M_t h}{b_{loc}}\right) \leq 0 \tag{46}$$

D. Constraint on the transmit power

Similar to that of point-to-point CRSN network in [11], it is assumed that each sensor node has maximum peak power constraint of 20 dBm which is equal to 100 mW. Similar constraint holds true even for proposed MIMO-CRSN architecture but because of the Alamouti encoding, the transmit power is equally spitted among the M_t transmit antennas corresponding to each node in the cluster. Although this scales down the received signal to noise ratio at the receiver but due to the inherent transmit diversity of the Alamouti encoding, there will be significant improvement in the performance which is shown through our extensive simulation results. Furthermore, in order to attain a specific average BER ($\overline{P_e}$), the required transmit power would depend on the modulation level (b) and packet size (l_s). Therefore, the transmit power constraint could be written as

$$c_3^{\mathbf{mimo}}(l_s, b, P_d, P_f, \overline{P_e}) = \frac{P_{out}^{\mathbf{mimo}}(l_s, b, P_d, P_f, \overline{P_e})}{M_t} - 0.1 \leq 0. \tag{47}$$

E. Constraint on the average BER

As modelled in point-to-point CRSN architecture, a constraint on the average BER $\overline{P_e}$ for our MIMO-CRSN architecture is considered. The rationale behind this is the fact that cognitive radio based network has various transmission sates

each with its own instantaneous BER based on the received SNR and SINR (discussed in the next section). To ensure a certain level of transmission reliability of the system and for the sake of mathematical simplification a constraint on the average BER is a reasonable technique that has already been established. For multihop scenario, the end to end average BER will turn out to be

$$1-(1-\overline{P_e})^{\overline{n}} \leq \overline{P_{eth}}, \tag{48}$$

where $\overline{P_e}$ is the average BER of each hop and $\overline{n}$ is the average number of hops. This must be less than or equal to a specific threshold $\overline{P_{eth}}$. In case of single hop the average BER will be simply $\overline{P_e} \leq \overline{P_{eth}}$.

F. The optimization problem

To guarantee protection of the non-cognitive users and to maximize the transmission opportunity by the cognitive users, the probability of detection $P_d \geq \tilde{P}_d$ and $P_f \leq \tilde{P}_f$ where $\tilde{P}_d = 0.9$ and $\tilde{P}_f = 0.1$ which is the benchmark as per any cognitive radio specifications. Based the on this and above subsections the optimization problem to determine the optimal packet size boils down to

$$\begin{aligned}
&\textbf{\textit{min}}_{b} && \textbf{\textit{max}}_{l_s}\ \eta_{\mathbf{mimo}}(l_s, b, P_d, P_f, \overline{P_e}, M_t) && \text{(49a)}\\
&\textbf{\textit{subject to}} && c_1^{\mathbf{mimo}}(l_s, b, P_d, P_f, M_t) \leq 0 && \text{(49b)}\\
& && c_2^{\mathbf{mimo}}(l_s, b, P_d, P_f, \overline{P_e}, M_t) \leq 0 && \text{(49c)}\\
& && c_3^{\mathbf{mimo}}(l_s, b, P_d, P_f, \overline{P_e}, M_t) \leq 0 && \text{(49d)}\\
& && \overline{P_e} \leq 1 - e^{\frac{1}{\overline{n}}\log(1-\overline{P_{eth}})} && \text{(49e)}\\
& && P_d \geq \tilde{P}_d && \text{(49f)}\\
& && P_f \leq \tilde{P}_f && \text{(49g)}\\
& && 100 < l_s < 1000, b \in \{2,3,4....10\}, && \text{(49h)}
\end{aligned}$$

where both b and l_s are discrete integers.

VI. Determination of the average BER under variablerate m-QAM and remodelling of the optimization problem

The transmit power (P_{out}) is determined based on the average BER $\overline{P_e}$. Therefore the energy consumption Average probability of error $\overline{P_e}$ will depend on the received SNR without interference from the non-cognitive user (γ_a) and received signal to interference and noise ratio which is the SINR (γ_b) both in terms of normalized bit energy to noise ratio $\frac{E_b}{N_0}$.

$$\gamma_a = ||H||_F^2 \frac{P_{rec}}{N_0 R} \tag{50}$$

$$\gamma_b = ||H||_F^2 \frac{P_{rec}}{(N_0 + P_{nc})R} \tag{51}$$

$$\gamma_b = \gamma_a \frac{N_0}{(N_0 + P_{nc})} \tag{52}$$

where P_{rec} is the received power from the cognitive transmitter to the cognitive receiver, P_{nc} is the power received at the cognitive receiver from the non-cognitive user as interference and g being instantaneous channel gain component with Rayleigh distribution. Again, since $R = bR_s$ therefore, both γ_a and γ_b will depend on the modulation level b. In Section III A, it is already shown that $\gamma_{pr} = \frac{\sigma_s^2}{\sigma_u^2}$ where σ_s^2 is the signal power received at the receiver end, $\sigma_u^2 = N_0 B$ is the total noise power where $\frac{N_0}{2}$ is single sided power spectral density and B is the bandwidth of the channel. Thus $\sigma_s^2 = \gamma_{pr}(N_0 B)$. σ_s^2 is now denoted as P_{nc} in this paper.

Power received at the cognitive receiver will depend upon the transmit power and the corresponding system and network configuration which includes the pathloss, link margin, antenna gains and system implementation losses etc. P_{rec} will be dependant on the transmit power and based on Friss law of pathloss, P_{rec} can be easily calculated to be as

$$\begin{aligned}
P_{rec_{\boldsymbol{dBm}}} &= P_{out_{\boldsymbol{dBm}}} + G_{t_{\boldsymbol{dB}}} + G_{r_{\boldsymbol{dB}}} + K_{pl_{\boldsymbol{dB}}} \\
&\quad - 10\delta \log_{10}\left(\frac{d_{ss}}{d_0}\right) - N_{f_{\boldsymbol{dB}}} - M_{l_{\boldsymbol{dB}}},
\end{aligned} \tag{53}$$

where $K_{pl} = 20\log_{10}\left(\frac{\lambda}{4\pi d_0}\right)$ is the pathloss component, G_t/G_r are the gains of the transmit and receive antennas, N_f is the noise figure, M_l is the link margin, δ is the pathloss exponent and $d_0 = 1\,m$ is the reference distance.

Taking the absolute value of the P_{rec} and substituting in (50) and (52) we can obtain the instantaneous SNR and SINR. Taking expectation operator $\mathbf{E}(\cdot)$ of γ_a and γ_b yields the average received SNR and SINR $\overline{\gamma_a}$ and $\overline{\gamma_b}$ which is used to estimate the average BER of the system.

As explained in the earlier section that the average BER is dependant on the probability of different cognitive transmission states, the instantaneous BER needs to to be calculated for different states where cognitive nodes transmits and the instantaneous BER has to be averaged over the pdfs of the received SNR and SINR to obtain the average BER. Let $\zeta(\gamma_a)$ and $\zeta(\gamma_b)$ be the corresponding BERs for the SNR (γ_a) and SINR (γ_b) respectively. Therefore, the instantaneous BER for different cognitive states can be estimated as

$$\begin{aligned}
Misdetection\,(\zeta_2):\ &\left(Pr_{on} + Pr_{off}e^{\frac{-l_s}{Rl_p}}\right)\zeta(\gamma_b) + \\
&Pr_{off}\left(1 - e^{\frac{-l_s}{Rl_p}}\right)\zeta(\gamma_a)
\end{aligned} \tag{54}$$

$$Co-selection\,(\zeta_4):\ \zeta(\gamma_b) \tag{55}$$

$$Collision\,(\zeta_5):\ Pr_{on}\zeta(\gamma_b) + Pr_{off}\zeta(\gamma_a) \tag{56}$$

$$Successful\,transmission\,(\zeta_6):\ \zeta(\gamma_a), \tag{57}$$

where $\zeta(\gamma)$, $\gamma \in \{\gamma_a, \gamma_b\}$ is the BER expression for the variable m-QAM modulation scheme given by

$$\zeta(\gamma) = \frac{4}{b}\left(1 - \frac{1}{2^{\frac{b}{2}}}\right) Q\left(\sqrt{\frac{3b}{(2^b-1)M_t}\gamma}\right) \tag{58}$$

Instantaneous BERs obtained in (54) to (57) needs to be weighted with the probabilities of its corresponding transmission states as shown in (13), (16) to (18). Therefore, the total instantaneous BER is calculated to be

$$\zeta_{total} = \frac{Pr_2\zeta_2 + Pr_4\zeta_4 + Pr_5\zeta_5 + Pr_6\zeta_6}{Pr_{on}(1-P_d) + Pr_{off}(1-P_f)}. \tag{59}$$

Substituting (54 to (57) in the above equation (59) and by simplifying we obtain

$$\zeta_{total} = \zeta(\gamma_a) + \Omega\left\{\zeta(\gamma_b) - \zeta(\gamma_a)\right\}, \tag{60}$$

where

$$\Omega = \frac{Pr_2(Pr_{on} + Pr_{off}e^{\frac{-l_s}{Rl_p}}) + Pr_4^{\mathbf{mimo}} + Pr_{on}Pr_5^{\mathbf{mimo}}}{Pr_{off}(1-P_f) + Pr_{on}(1-P_d)}. \tag{61}$$

The total instantaneous BER will turn out to be

$$\zeta_{total} = \frac{4}{b}\left(1 - \frac{1}{2^{\frac{b}{2}}}\right)\left[(1-\Omega)\left\{Q\left(\sqrt{\frac{3b}{(2^b-1)M_t}\gamma_a}\right)\right\} + \Omega\left\{Q\left(\sqrt{\frac{3b}{(2^b-1)M_t}\gamma_b}\right)\right\}\right], \tag{62}$$

The average BER of the MIMO-CRSN system will be

$$\overline{P_e} = \mathbf{E}_\gamma\left(\zeta_{total}\right), \tag{63}$$

where $\mathbf{E}(\cdot)$ is the expectation operator.

Therefore, the average BER $(\overline{P_e})$ turns out to be

$$\overline{P_e} = \frac{4}{b}\left(1 - \frac{1}{2^{\frac{b}{2}}}\right)\left[(1-\Omega)\,\mathbf{E}_{\gamma_a}\left\{Q\left(\sqrt{\frac{3b}{(2^b-1)M_t}\gamma_a}\right)\right\} + \Omega\mathbf{E}_{\gamma_b}\left\{Q\left(\sqrt{\frac{3b}{(2^b-1)M_t}\gamma_b}\right)\right\}\right], \tag{64}$$

where from [41], [42].

$$\mathbf{E}_\gamma\left\{Q\left(\sqrt{\frac{3b}{(2^b-1)M_t}\gamma}\right)\right\} = \left[\frac{1}{2}\left\{1 - \sqrt{\frac{\frac{3b\gamma}{(2^b-1)M_t}}{2+\frac{3b\gamma}{(2^b-1)M_t}}}\right\}\right]^L \sum_{i=0}^{L-1}\frac{1}{2^i}\binom{L-1+i}{i}\left\{1 - \sqrt{\frac{\frac{3b\gamma}{(2^b-1)M_t}}{2+\frac{3b\gamma}{(2^b-1)M_t}}}\right\}^i, \tag{65}$$

In the above equation (65), $L = (M_t \times N_r)$ which is the diversity order. For $\gamma \in \{\gamma_a, \gamma_b\}$ taking into account the Frobenius norm of the MIMO channel matrix [42]. In our simulation

Since $\gamma_a >> 1$ and $\gamma_b > 1$ at very high values of γ_a

$$\mathbf{E}_\gamma\left\{Q\left(\sqrt{\frac{3b}{(2^b-1)M_t}\gamma}\right)\right\} = \binom{2L-1}{L}\frac{1}{2^L}\left\{\frac{3b}{(2^b-1)M_t}\gamma\right\}^{-L} \tag{66}$$

$$\overline{P_e} \approx \frac{4}{b}\left(1 - \frac{1}{2^{\frac{b}{2}}}\right)\binom{2L-1}{L}\frac{1}{2^L}\left(\frac{3b}{(2^b-1)M_t}\gamma_a\right)^{-L}\left\{1 + \Omega\left(\left[\frac{N_0+P_{rp}}{N_0}\right]^L - 1\right)\right\} \tag{67}$$

$$\gamma_a = \left[\frac{1}{\overline{P_{eth}}}\frac{4}{b}\left(1 - \frac{1}{2^{\frac{b}{2}}}\right)\binom{2L-1}{L}\frac{1}{2^L}\left(\frac{3b}{(2^b-1)M_t}\right)^{-L}\left\{1 + \Omega\left(\left[\frac{N_0+P_{rp}}{N_0}\right]^L - 1\right)\right\}\right]^{\frac{1}{L}} \tag{68}$$

From (36), (37) and (61), since Ω is a function of packet size l_s therefore, the the average BER $(\overline{P_e})$ will be a function of packet size. Furthermore, it is also observed that Ω depends on the probability of detection (P_d) and probability of false alarm P_f (61) . It has been shown by the authors of [37] that for a given probability of detection threshold P_d, the probability of false alarm (P_f) will b a monotonically decreasing function with respect to the channel sensing time τ_s. Since our network is a delay sensitive network and longer channel sensing duration consumes additional overhead energy (14), the probability of detection and false alarm is fixed to a specific threshold $\tilde{P_d}$ and $\tilde{P_f}$ and treat them as equalities instead of the inequalities as shown in the constraints of the formulated optimization problem (49f) and (49g). This essentially leads to further simplification of the the optimization problem.

Using the equation above, now we can easily calculate the received SNR at the cognitive receiver and the corresponding transmit power required to attain specific BER threshold of $\overline{P_{eth}}$ from (53) and (66),

$$P_{out}(l_s, b, \tilde{P_d}, \tilde{P_f}, \overline{P_{eth}}, M_t, N_r) \leq \frac{(4\pi)^2 d_{ss}^{\delta} M_l N_f}{G_t G_r \lambda^2}\gamma_a N_0 R. \tag{69}$$

Similarly, since energy consumed per bit (k_1) is depending directly on the transmit power P_{out}. From (35) and (67),

$$k_1(l_s, b, \tilde{P_d}, \tilde{P_f}, \overline{P_{eth}}) \leq \left\{(1+\alpha)P_{out} + P_c\right\}\frac{1}{R} \tag{70}$$

The initial cost function (36) now becomes,

$$\eta_{\mathbf{mimo}} = \frac{\boldsymbol{k_1(l_s, b, \tilde{P_d}, \tilde{P_f}, \overline{P_{eth}}, M_t, N_r)}(l_s - M_t h)(1-\overline{P_{eth}})^{M_t l_s}}{\boldsymbol{(k_1(l_s, b, \tilde{P_d}, \tilde{P_f}, \overline{P_{eth}}, M_t, N_r)} + k_{loc})l_s + E_{tot}(\tilde{P_d}, \tilde{P_f})} \tag{71}$$

Finally, taking into account a fixed average BER threshold $\overline{P_e} = \overline{P_{eth}}$ and expressing the energy consumption per bit k_1 as a function of P_{eth}, the simplified optimization problem boils down to

$$\begin{aligned}
&\underset{b}{\textbf{\textit{min}}} && \underset{l_s}{\textbf{\textit{max}}}\ \eta_{\mathbf{mimo}}(l_s, b, \tilde{P}_d, \tilde{P}_f, \overline{P_{eth}}, M_t, N_r) && \text{(72a)}\\
&\textbf{\textit{subject to}} && c_1^{\mathbf{mimo}}(l_s, b, \tilde{P}_d, \tilde{P}_f, M_t) \leq 0 && \text{(72b)}\\
& && c_2^{\mathbf{mimo}}(l_s, b, \tilde{P}_d, \tilde{P}_f, \overline{P_{eth}}, M_t, N_r) \leq 0 && \text{(72c)}\\
& && c_3^{\mathbf{mimo}}(l_s, b, \tilde{P}_d, \tilde{P}_f, \overline{P_{eth}}) \leq 0 && \text{(72d)}\\
& && 100 < l_s < 1000, b \in \{2, 3, 4....10\}\,, && \text{(72e)}
\end{aligned}$$

where both b and l_s are discrete integers.

VII. Algorithms to determine the optimal packet size

A. Exhaustive Search Based Algorithm-1

An exhaustive search based Algorithm-1 is proposed to solve the formulated optimization problem (72a) to (72e). As both modulation level (b) and packet size (l_s) are discrete integers, the energy consumption per bit k_1 and all the other constraints $c_1^{\mathbf{mimo}}$, $c_2^{\mathbf{mimo}}$ and $c_3^{\mathbf{mimo}}$ related to the interference duration, end-to-end delay and peak transmit power constraints are calculated based on (72b), (72c) and (72d) for all the of the packet sizes ranging from $l_s = \{100, 101, ...1000\}$ bits and for a specific modulation level (b). Based on the feasibility of all the three constraints, and optimal packet length l_s^* is obtained which would maximize the cost function (72a). The value of the cost function at l_s^* is denoted as $\eta_{\mathbf{mimo}}^*$. Same process is repeated for a range of modulation levels (b) supported by the variable rate m-QAM modulation scheme where b ranges from $b = \{2, 3, 4, ...9\}$. Once the values of the

maximized cost function for each b is obtained, the minimum $\eta_{\mathbf{mimo}}^*$ is selected and its corresponding l_s^* and b provides the optimal packet size and modulation level.

B. Conventional Karush-Kuhn-Tucker (KKT) based algorithm

An efficient suboptimal algorithm based on solving the Karush-Kuhn-Tucker conditions denoted as Algorithm-2 is proposed to solve the optimization problem. In Algorithm-2 the packet size l_s is considered to be continuous unlike Algorithm where it was considered to be discrete in nature. For the next step, the cost function in this technique is modified to a new Lagrangian function which comprises of the original cost functions and the constraint functions which is now multiplied by the lagrangian multipliers λ_1, λ_2 and λ_3 corresponding to the three constraint functions (72b), (72c) and (72d). The root of derivative of this newly formed Lagrangian function with respect to the decision variable (l_s) needs to be calculated. Furthermore, along with the lagrangian function, the feasibility of the constraint functions, the complimentary slackness condition related to the lagrangian variable and the constraints and the negativity of the lagrangian conditions needs to be satisfied which provided what is known as the feasible KKT point. Negativity condition of the Lagrangian multipliers is because in our case for each modulation level, the original cost function is a maximization problem.

For each of the modulation level, the feasible KKT point is searched and the root for the modified cost function is obtained using classical Newton-Raphson assisted numerical technique.

Algorithm-1 Exhaustive Search to determine OPS for MIMO-CRSN .

Require: l_s^{opt}, b^{opt}
Initialize: $l_s = \{100, 101, ...1000\}$, $b = \{2, 3, 4...9\}$, $\tilde{P}_d = 0.9$, $\tilde{P}_f = 0.1$, $\overline{P_{eth}}$, *ii*= 1, *jj*= 1.
for *ii*=1 to $max(b)$ **do**
  for *jj*=1 to $max(l_s)$ **do**
    Calculate: $\eta_{\mathbf{mimo}}(l_s(jj), b(ii), \tilde{P}_d, \tilde{P}_f, \overline{P_{eth}}, M_t)$ from (72a)
    $c_1^{\mathbf{mimo}}(l_s(jj), b(ii), \tilde{P}_d, \tilde{P}_f, \overline{P_{eth}}, M_t)$ from (72b)
    $c_2^{\mathbf{mimo}}(l_s(jj), b(ii), \tilde{P}_d, \tilde{P}_f, \overline{P_{eth}}, M_t)$ from (72c)
    $c_3^{\mathbf{mimo}}(l_s(jj), b(ii), \tilde{P}_d, \tilde{P}_f, \overline{P_{eth}}, M_t)$ from (72d)
  end for
  Find: Set of l_s values $(\overline{l_s})$ for which both $c_1^{\mathbf{mimo}}(l_s) \leq 0$ and $c_2^{\mathbf{mimo}}(l_s) \leq 0\ \forall \overline{l_s}$ at $b = b(ii)$
  if $\overline{l_s}$ exist **then**
    Find: $\{l_s^{max} : l_s^{max} = l_s \hat{=} max(\eta_{\mathbf{mimo}})\}$ at b=b(ii)
    if $c_3^{\mathbf{mimo}}(l_s^{max}, b(ii)) \leq 0$ **then**
      $l_s^*(ii) = l_s^{max}$
      $\eta_{\mathbf{mimo}}^*(ii) = max(\eta_{\mathbf{mimo}})$
    else if $c_3^{\mathbf{mimo}}(l_s(1), b(ii)) > 0$ **then**
      $l_s^*(ii) = \times$
      $\eta_{\mathbf{mimo}}^*(ii) = \times$
    else
      Find: Set of l_s values $(\overline{l_s}^p)$: $\overline{l_s}^p \in \overline{l_s}$ and $c_3^{\mathbf{mimo}}(l_s) \leq 0\ \forall \overline{l_s}^c$ at $b = b(ii)$
      $l_s^*(ii) = \overline{l_s}^p(end)$
      $\eta_{\mathbf{mimo}}^*(ii) = \eta_{\mathbf{mimo}} \hat{=} l_s^*$
    end if
  else
    $l_s^*(ii) = \times$
    $\eta_{\mathbf{mimo}}^*(ii) = \times$
  end if
end for
Find: $\eta_{\mathbf{mimo}}^{min} = min(\eta_{\mathbf{mimo}}^*)$
Find: $l_s^{opt} : l_s^{opt} = l_s^* \hat{=} \eta_{\mathbf{mimo}}^{min}$
Find: $b^{opt} : b^{opt} = b \hat{=} l_s^{opt}$

For each of the modulation level (b), the KKT point and its corresponding value of the original cost function $(\eta_{\mathbf{mimo}})$ is found. Finally, just like Algorithm-1 the value of the KKT point corresponding to the minimum $(\eta_{\mathbf{mimo}})$ or k_1 value provides optimal packet size L^{opt}.

$$\frac{\partial L(l_s, \lambda_1, \lambda_2, \lambda_3)}{\partial l_s} = \frac{\partial \eta_{\mathbf{mimo}}(l_s)}{\partial l_s} + \lambda_1 \frac{\partial c_1^{\mathbf{mimo}}(l_s)}{\partial l_s} + \lambda_2 \frac{\partial c_2^{\mathbf{mimo}}(l_s)}{\partial l_s} + \lambda_3 \frac{\partial c_3^{\mathbf{mimo}}(l_s)}{\partial l_s} = 0 \tag{73}$$

$$\begin{cases}
\left.\begin{aligned} c_1^{\mathbf{mimo}}(l_s) \leq 0 \\ c_2^{\mathbf{mimo}}(l_s) \leq 0 \\ c_3^{\mathbf{mimo}}(l_s) \leq 0 \end{aligned}\right\} \rightarrow Feasibility & \text{(74a)}\\
\left.\begin{aligned} \lambda_1 c_1^{\mathbf{mimo}}(l_s) = 0 \\ \lambda_2 c_2^{\mathbf{mimo}}(l_s) = 0 \\ \lambda_3 c_3^{\mathbf{mimo}}(l_s) = 0 \end{aligned}\right\} \rightarrow Compl.\ \ Slackness & \text{(74b)}\\
\left.\begin{aligned} \lambda_1 \leq 0 \\ \lambda_2 \leq 0 \\ \lambda_3 \leq 0, \end{aligned}\right\} \rightarrow Negativity & \text{(74c)}
\end{cases}$$

Fig. 3 shows the schematic representation of Algorithm-2 with different subalgorithms illustrated in the appendix.

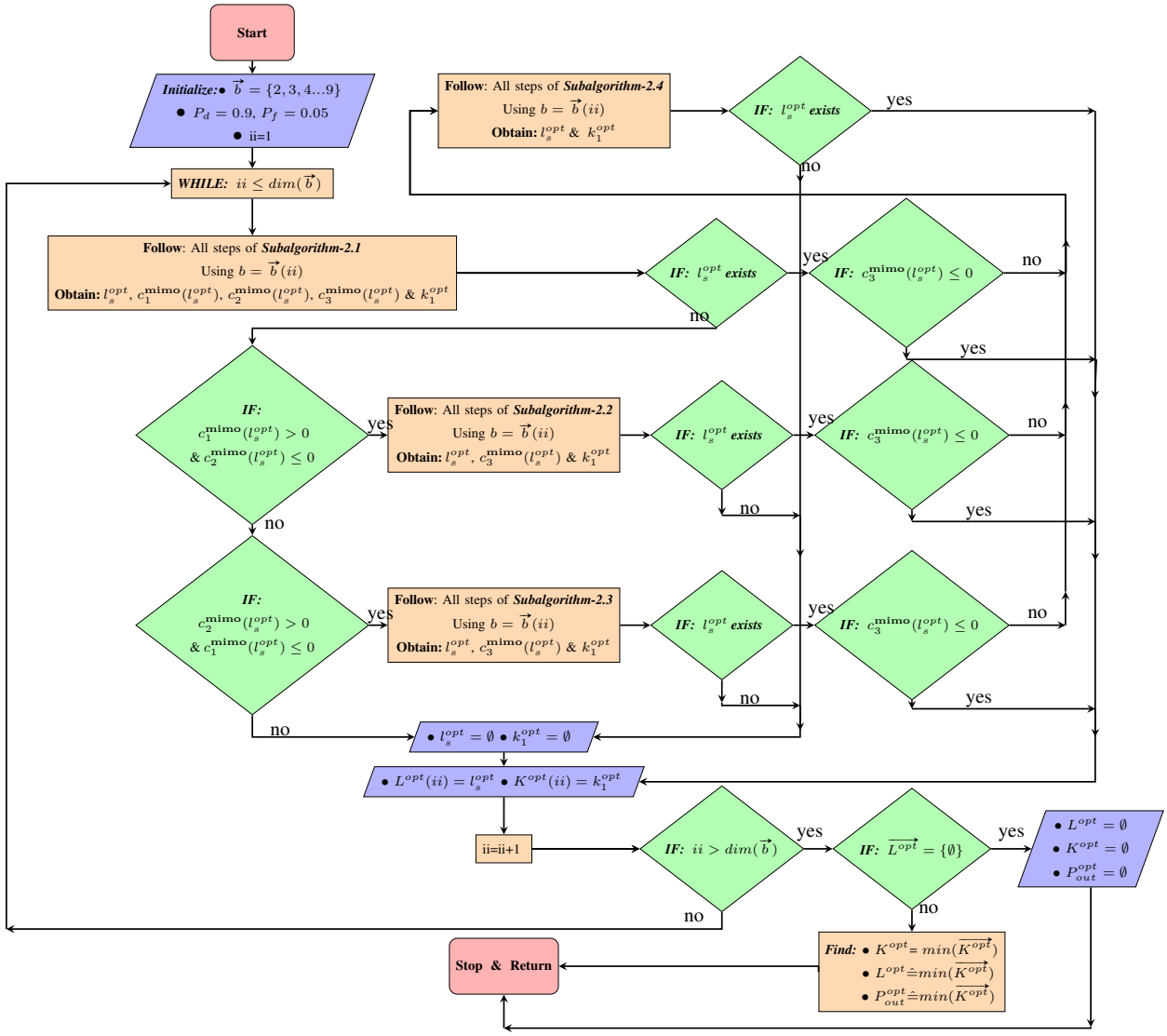

Fig. 3. Newton-Raphson technique assisted KKT-based **Algorithm-2** [11]

VIII. NUMERICAL RESULTS

Table I. SIMULATION PARAMETERS

Symbol	Definition	Value
B	Channel Bandwidth	1 MHz
f	Operating Frequency	2.4 GHz
Pr_{on}	probability of primary occupancy	$\frac{1}{2}$ $\frac{1}{3}$
v_p	avg. channel idle time	200 ms
d_{ss}	distance between two cognitive secondary users	10 m
b	bits/symbol for m-QAM	{ 2,3...9 }
R_s	fixed symbol rate	10 bauds
δ	path-loss exponent	2,2.5,3
$G_t G_r$	Gain of the transmitter and receiver of secondary users	5 dBi
M_l and N_f	link margin and noise figure	5 dB and 10 dB
P_{ctx}	Power consumed by the transmitter circuit	98.3 mw
P_{crx}	Power consumed by the receiver circuit	125 mw
N_0	one sided thermal noise	-171 dBm/Hz
$header(h)$	size of the header in bytes	6 bytes
P_{sens}	power consumed by the circuit due to channel sensing	110 mw
E_{hf}	energy consumed during hand-off	2 mJ
k_{loc}	local energy consumption per bit at T_x	5μJ, 2μJ
N_r	No. of receiver antennas or receivers at the intermediate R_x cluster	1

In Fig. 4(a), the optimal packet size values versus increasing number of users in system (M) is compared for different interference levels from the non-cognitive users. Probability of occupancy by the non-cognitive users (Pr_{on}) is assumed to be $\frac{1}{3}$ and distance d_{ss}= 10 m. (2×1) MIMO-CRSN architecture is considered and the optimal packet size is estimated using both exhaustive search based Algorithm-1 and KKT based Algorithm-2. Furthermore, the results are compared to cognitive point-to point system. Distributed time slotted channel access is considered for the results. It could be observed that there is a perfect match among the simulation results obtained using Algorithm-1 and Algorithm-2. Furthermore, for both the MIMO-CRSN and P2P-CRSN system, the OPS value decreases with the increase in the number of users. However, as compared to the P2P system in case of MIMO based CRSN network, the decrease in the OPS value is not very high for different values of the interference level SNR_{pr}. At SNR_{pr}= -10 dB, the OPS value for M=6 users for MIMO-CRSN system is 290 bits while as the number of users is increased to 20, the OPS value turns out to be 287 bits. Under similar

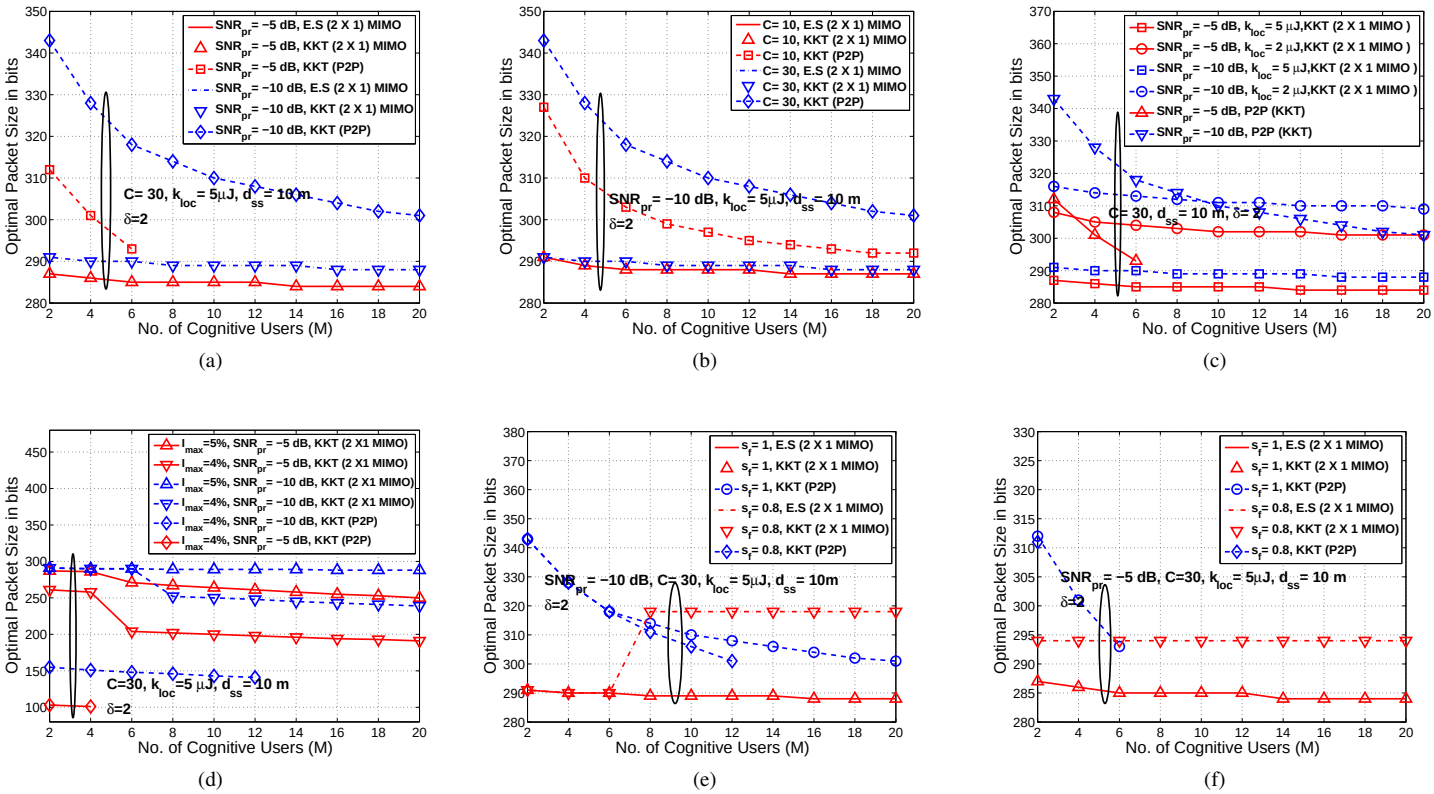

Fig. 4. Optimal packet size in bits (OPS) versus varying number of cognitive secondary users (M) with proposed E.S and KKT algorithms . a. For varying interference power (SNR_{pr}), b. For varying number of channels (C), c. For varying energy consumption per bit for local intracluster communcation k_{loc}, d. For varying percentage of interference duration to nc-users (I_{max}) e. For varying delay sharpening factor (s_f), at SNR_{pr}= -10 dB f. For varying delay sharpening factor (s_f), at SNR_{pr}= -5 dB

scenario for P2P-CRSN system, OPS value at M=6 turns out to be 318 bits while at M=20 it will be 301 bits. This is due to the fact that with the increase in the number of users in the system results in increase of the energy consumption per bit k_1 both for the MIMO and P2P CRSN system alike (70). Since it is already proven that the cost function η will be an increasing function of k_1. For a fixed value of l_s, the value of the cost function which is the energy-efficiency reliability metric increases and the optimal l_s for which the cost function gets maximized reduces with increasing k_1. This leads to a sharp decline in the OPS value or P2P-CRSN architecture but for MIMO-CRSN system, the cost function $\eta_{\mathbf{mimo}}$ (72a) apart from the k_1 component also contains the overhead energy consumption at the transmitter end due to local intracluster information exchange to enable Alamouti encoding. This significant overhead energy consumption component in the denominator of the cost function scales down the cost function and the rate of decrease in the OPS value with increasing k_1 or M is not as high as compared to P2P-CRSN system. Similar trend could be observed when the network conditions are made severe with increased interference level SNR_{pr}= -5 dB. However OPS value for P2P-CRSN could be obtained only upto 6 users beyond which the peak power constraint of 20 dBm for each sensor node could not be satisfied to meet the average BER threshold $\overline{P_{eth}}$= 10^{-3}. In case of MIMO-CRSN since the transmit power is divided equally among the two M_t= 2 sensor nodes, optimal packer size could easily obtained upto 20 users in system with OPS values ranging from 287 to 284 bits at M=2 and M= 20 users.

Fig. 4(b), shows the OPS value for the MIMO-CRSN and P2P-CRSN architecture for increasing number of cognitive users in the system for different number of available channels (C) for a fixed interference power SNR_{pr}= -10 dB. In case of (2×1) MIMO-CRSN system as the number of available channels is reduced from C=30 to $C = 10$, a marginal reducing in the OPS value could be observed. Whereas in P2P-CRSN the reduction in the OPS value for reducing the number of channels from 30 to 10 is quite significant. At M=10, the OPS value when C=30 is around 310 bits and OPS value is 297 bits when C=10. The reason is contributed by the fact that decrease in the number of channels leads to increased Co-selection probability (4) as chances of more than single cognitive user selecting the same channel for data transmission increases. This leads to increases k_1 to attain a specific BER threshold thus reducing the optimal packet size length. However, just like Fig. 4(a), the reason for marginal decrease in the OPS value for MIMO-CRSN is due to the intracluster local energy consumption overhead. Even though marginal but the reason for decrease in the OPS value for decrease in channel numbers for MIMO-CRSN is same to that of point-to point CRSN. Moreover, again in this figure it could be observed that the results obtained from Algorithm-1

and Algorithm-2 are perfect match.

The OPS values for different intracluster communication energy requirement k_{loc} is analyzed in Fig. 4(c). The motivation for such analysis is due to the varied mean intracluster distance among the sensor nodes. Higher intracluster distance value leads to higher local energy consumption per bit k_{loc}= 5 μJ and for shorter mean distance it could be as low as 2 μJ Two different values of k_{loc} fixed at 5 μJ and 2 μJ are considered based based on which the OPS value are estimated at SNR_{pr}= -10 dB and SNR_{pr}= -5 dB respectively. It could be observed that when k_{loc} is 2 μJ, the OPS values are higher than that of k_{loc}= 5μJ both at SNR_{pr}= -10 dB and -5 dB. This is due to the fact $k_{loc} << k_1$ and it is absolutely independent of the long haul enegy consumption per bit k_1 as it is assumed that communication for local intracluster information exchange takes place among channels which is not accessed by the non-cognitive users. As the k_{loc} value gets higher for a fixed k_1 and l_s, the nature of the overall cost function η_{bfmimo} is dominated by the k_{loc}. As the k_{loc} gets higher from 2 μJ to 5 μJ, the value of the cost function for each packet length scales down. However, in this case as the cost function reduces, the optimal packet length l_s which would maximize the cost function would decrease unlike the previous results in Fig. 4(a) and Fig. 4(b) where increasing cost function value with increasing k_1 would lower the optimal packet size value.

In Fig. 4(d), the OPS value for different number of cognitive users are shown for two different values of maximum interference duration to non-cognitive users threshold I_{max} at 5% and 4% respectively. Comparison is made both (2×1) MIMO-CRSN system and well as point- to-point CRSN system. It could be observed that for both the SNR_{pr} values at -10 dB and -5 dB, there is a sharp decline in the OPS values when the interference constraint duration constraint that is $c_3^{\mathbf{mimo}}$ (72d) is made active and more severe. If we compare the results of Fig. 4(d) with Fig. 4(a), when the interference constraint is inactive as in Fig. 4(a), for the MIMO-CRSN system the OPS values at SNR_{pr}= -10 dB ranges from 292 to 287 while for SNR_{pr}= -5 dB it varies from 287 to 285 when M is varying between 2 to 20 users. Under the influence of the constraint, this results sharply falls to 250 to 200 bits when for SNR_{pr}=-5 dB when $I_{max} = 4\%$ and 287 to 248 bits at SNR_{pr}= -10 dB at I_{max} equal to 4%. Futhermore, when compared with point-to-point CRSN system, OPS could be determined only upto 12 users at SNR_{pr}= -10 dB and only 2 users at SNR_{pr}= -5 dB with lower values at around 150 bits and 100 bits. This is caused because of the fact that in MIMO-CRSN system, the total number of users actually contending over C data channels is scaled down by the number of users present in each MIMO cluster (M_t) as these M_t users in each cluster will transmit over the same channel. Thus the contention is reducen in MIMO-CRSN system.

Fig. 4(e) and Fig. 4(f) the OPS values are shown for varying delay sharpening factor s_f at SNR_{pr}= 10 dB and -5 dB. As total end to end delay $\tau_d = \frac{s_f MK}{R_s}$ where R_s is the fixed symbol rate, reducing s_f leads to reduction of the time duration τ_d thus making the delay constraint more severe. It could be observed that when s_f is reduced from 1 to 0.8 at SNR_{pr}= -10 dB, in case of (2) MIMO-CRSN scenario, the OPS value remains same upto 6 users both for $s_f = 1$ and $s_f = 0.8$ around 290 bits but as number of cognitive users (M) in the system increases, the OPS value for $s_f = 0.8$ increases to 318 bits and saturates. This is because as long a $s_f = 1$ and M=6, the delay constraint is not active and the results obtained is similar to that of OPS values in Fig. 4(a). However, as s_f is reduced to 0.8 the delay constraint $(c_2^{\mathbf{mimo}})$ becomes active for users above 6. This leads to higher packet size as in this case the optimal packet size will be determined by the constraint function and not necessarily the packet size which would maximized the cost function as in other cases described. When this result is compared with point-to-point CRSN architecture, it could be also observed that under $s_f = 0.8$, OPS could be obtained only upto 12 users in the system as to MIMO-CRSN which enables to determine OPS for 20 users. This is because MIMO-CRSN selects higher modulation level as compared to P2P-CRSN. Furthermore, in this case too the results obtained from exhaustive search based Algorithm-1 and KKT based Algorithm-2 provides a perfect match which proves the mathematical accuracy of our proposed algorithms under active constraint cases. For Fig. 4(f), as the SNR_{pr} is made more severe to -5 dB, the trends of the results remains same with only difference being now at $s_f = 0.8$, the OPS saturates at 294 bits when M=2.

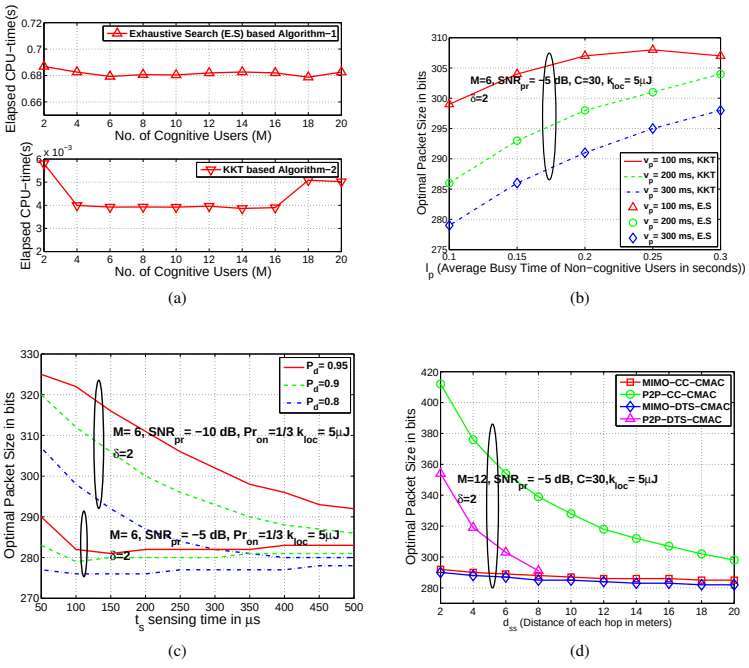

Fig. 5. a. Elapsed CPU time versus no.of cognitive users (M) for Algorithm-1 and 2 b. OPS versus the average busy time at M=6, SNR_{pr}= -5 dB for different values of v_p, c. OPS versus channel sensing time at M=6, SNR_{pr}= -5/-10 dB for different values of P_d, d. OPS versus varying distance for different distributed and centralize channel access schemes at SNR_{pr}= -5 dB, M=12.

Fig. 5(a) is one of the significant result shown in this paper. The performances of Algorithm-1 and Algorithm-2 in terms of the elapsed CPU time for different users is shown in this result for a (2×1) MIMO-CRSN architecture. Considering the NP hard nature of the optimization problem, the proposed

algorithms based on exhaustive search (Algorithm-1) and Newton-Raphson numerical technique assisted conventional KKT based (Algorithm-2) are heuristic in nature and a straight forward analysis of its order of complexity in trivial. However,

a rather indirect approach to estimate the performance of the proposed algorithms is to use the MATLAB command ***CPUTIME*** which shows a rough estimate of the time consumed by the CPU during simulation to execute Algorithm-1 and Algorithm-2 for a given number of users in the system. Although, this estimation technique depends upon numerous factors like the type of computer processor used during the simulation (Intel I5 in our case) etc. however, the mentioned approach helps us to evaluate and have a holistic overview of the performance of the proposed algorithms. The elpased CPU-time is this case is estimated for 10000 simulation seeds and then the average is calculated. It could be observed that Algorithm-2 takes 4 ms to obtain the optimum packet size while for Algorithm-1 the time taken is in the order of 680 ms. This is contributed by the fact that for exhaustive search technique, the search space spans over all the discrete values of packet length that is $l_s = \{100, 101....2000\}$ and modulation level $b = \{2, 3, 4..9\}$. The cost function and the constraint functions derived from (72a) to (72d) are calculated for all the l_s and b values discretely to check the feasibility and determination of the OPS. The elapsed time duration could be shortened though by reducing the search space upon the application but however in case of Algorithm-2, the search calculation depends upon the number of iterations of the Newton-Raphson Algorithm to find the root of the lagrangian based modified cost function (83) to determine the OPS. Furthermore, to determine the feasibility considering the constraint functions, the lagrangian variables of the formulated KKT solution and mathematically simplified constraint functions as shown in (88) to (95), helps to determine the feasible optimal point without discretely checking each and every packet length to determine the OPS.

In Fig. 5(b), the OPS value is shown for varying average busy time l_p and average idle time v_p of the non-cognitive users for MIMO-CRSN system for a given number of users in the system M=6. With increase in l_p from 100 to 300 ms for average idle time v_p fixed at 100, 200 and 300 ms, the packet size increases. This is because as l_p is increasing, the probability of occupancy Pr_{on} of the non-cognitive users increases. With increasing Pr_{on}, the energy consumed due to channel switching increases significantly which scales down the cost function and the size which maximizes the cost function $(\eta_{\mathbf{mimo}})$ increases. This counterintuitive result hold true even for point to point CRSN system as shown in our previous work [11]. Similarly as v_p increases from 100 ms to 300 ms, the Pr_{on} decreases since $Pr_{on} = \frac{l_p}{(l_p+v_p)}$. Therefore, for a fixed l_p, the OPS value will be maximum when v_p= 100 ms. Results ousing Algorithm-1 and Algorithm-2 shows perfect match. Fig. 5(c) shows the OPS values for different probability of detection P_d and channel sensing time τ_s for fixed number of cognitive users in the system M= 6 and $Pr_{on} = \frac{1}{3}$ at SNR_{pr}= -10 dB and -5 dB. With increasing sensing time from 50 μs to 500 μs, the OPS value decreases for a fixed P_d value when SNR_{pr}= -10 dB. This trend is different than the results shown in [11]. The reason for decrease in OPS value with increasing sensing time is due to the fact that at higher channel SNR at around -10 dB, the channel sensing time is of the order of micro seconds which is very low. However, as channel sensing time t_s increases the probability of false alarm P_f would decrease monotonically for a fixed P_d value. This decrease in the probability of false alarm results into decrease in the overhead energy consumed due to channel handoff (E_{hf}) as probability of channel switching (P_{sw}) decreases. This leads to an increase in the cost function $\eta_{\mathbf{mimo}}$ as E_{hf} is in the denominator of the cost function. Therefore, the packet size now at which the cost function will be maximized will reduce as t_s would increase which leads to lower packet size. When the SNR_{pr} is made more severe at -5 dB, the OPS value will saturate beyond 120 μs. This is because with increased value of SNR_{pr}= -5 dB, the effect of increasing sensing time will have minimum impact on the probability of false alarm. Therefore, the OPS value will not reduce any further beyond a specific t_s. In Fig. 5(d), the behaviour of the OPS with varying transmission distance is analyzed for two different access schemes based on MIMO distributed time slotted medium access control denoted as MIMO-TS-CMAC and a CSMA/CA assisted centralized common control channel based medium access control denoted as MIMO-CC-CMAC and the same is compared with point-to point CRSN system with distributed and centralized access schemes. Under severe network conditions when SNR_{pr}= -5 dB and the number of cognitive users in the system M=12, it could be observed that distributed MIMO-CRSN system outperforms the single point-to point distributed CRSN system as OPS could be obtained only upto 8 m in a point to point scenario. However, the packet size for both the cases would reduce as the transmission distance increases since energy consumption per bit k_1 would increase with increasing distance and the OPS would naturally decrease. The OPS value for P2P-DTS-CMAC will be lesser than that of P2P-CC-CMAC as in the centralized system the probability of co-user selection does not exist which negates the risk of more than one cognitive user selecting the same data channel. This reduces the k_1 value for the centralized system thus providing higher OPS values. Same arguments holds true for the MIMO-CRSN scenario however, this OPS gap will not be significant due to additional overhead energy consumed due to local information exchange as k_{loc} is fixed at 5 μJ.

In Fig. 6(a) and Fig. 6(b),the overall energy consumption of the system is shown for a (2×1) MIMO based distributed time slotted cognitive channel access scheme (MIMO-DTS-CMAC) for varying transmission distance at SNR_{pr}= 10 dB and SNR_{pr}= -5 dB. When SNR_{pr}= -10 dB. Moreover, the results are compared with cognitive point-to-point CRSN system with distributed access scheme. In Fig. 6(a), the overall energy consumption is shown for two test cases when number of cognitive users in the system M= 6 and M= 12. It could be observed that for increasing transmission distance from 2 to 20 m the overall energy consumption will increase both for MIMO and P2P CRSN framework which is quite obvious. However, the MIMO-DTS-CMAC with optimal packet size

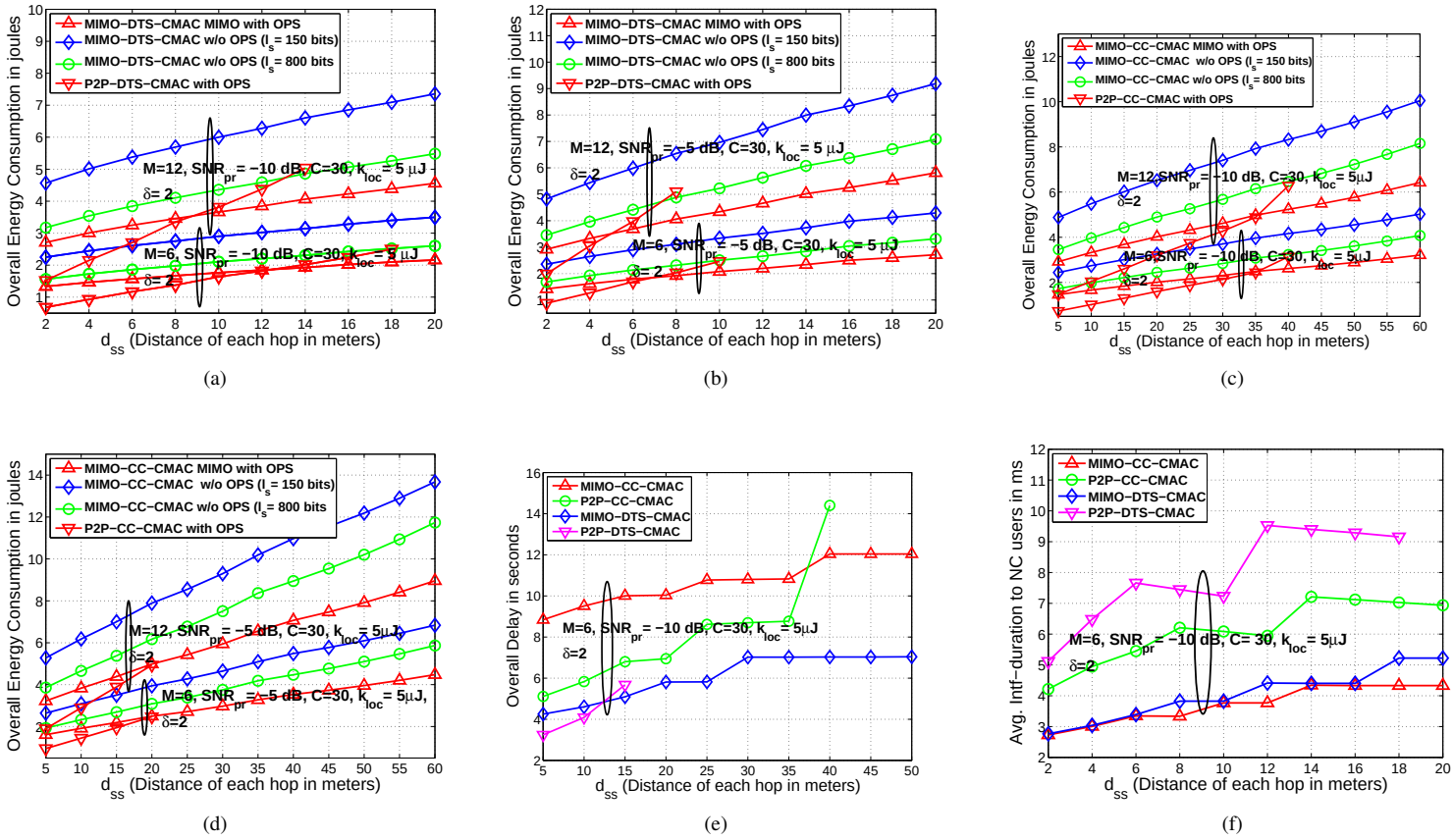

Fig. 6. Overall energy consumption versus varying distance for MIMO and P2P mode for DTS-CMAC for a. SNR_{pr}= -10 dB, b. SNR_{pr}= -5 dB, Overall energy consumption versus varying distance for MIMO and P2P mode for CC-CMAC for c. SNR_{pr}= -10 dB, d. SNR_{pr}= -5 dB, e. Overall delay versus varying distance for distributed and centralized access schemes for MIMO and P2P mode with OPS at SNR_{pr}= -10 dB . f. Overall delay to nc-users versus distance for distributed and centralized access schemes for MIMO and P2P mode with OPS at SNR_{pr}= -10 dB

is compared with a fixed packet MIMO-CRSN system with packet size (l_s) being fixed at 150 bits and 800 bits. It could be be observed that both for M= 6 and M= 12, the (2×1) MIMO-DTS-CMAC with OPS will outperform the P2P-DTS-CMAC system with OPS only beyond a critical distance threshold which is 10 m in this case. This due to the overhead energy consumption caused due to intracluster communication. Furthermore, both the fixed packet size based MIMO-CRSN schemes will have higher energy consumption as compared to the MIMO-CRSN based system with OPS which helps us to envisage the usefulness of transmitting with an optimal packet size for the proposed MIMO-CRSN system. The similar trend holds true when M is increased to 12 users. Another interesting observation is P2P-CRSN system could support optimal packet size only upto d_{ss}= 14 m above whicha feasible optimal packet length could not be obtained due to the transmit power constraint. Fig. 6(b) shows similar results to that of Fig. 6(a) with only difference being the critical distance beyond which MIMO-DTS-CMAC with OPS outperform P2P-CRSN system with OPS is further reduced to 8 m and 6 m when M= 6 and 12 respectively. For Fig. 6(c) and Fig. 6(d), a CSMA/CA dependent (2×1) MIMO based centralized common control channel assisted cognitive medium access control (MIMO-CC-CMAC) is considered [39]. The trends of the results are similar to that of the last two figures but however, the critical distance beyond which the MIMO-CC-CMAC outperforms the P2P-CC-CMAC system beyond 35 m both for M= 6 and M= 12 at SNR_{pr}= -10 dB while at SNR_{pr}= -5 dB the critical distance would be 20 m beyond which OPS could not be obtained for the centralized point-to-point system. Furthermore, if we carefully examine the results obtained from the distributed system and compare it with the centralized MIMO based access scheme, the overall energy consumption will be lesser for the centralized system as multiple cognitive users does not selects the same channel. In Fig. 6(e), the overall end to end delay analysis is shown for the two aforementioned channel access schemes both for the proposed MIMO-CRSN system and point-to-point system with OPS. It could be observed that in terms of overall delay for point to point system with optimal packet size will be lower than any of the MIMO based CRSN system upto a critical distance of 37 m for the centralized system and 13 m for the distributed system beyond which delay for the P2P mode will increase and and further no feasible optimal packet size could be obtained. This is mainly due to the overhead delay caused due to the local information exchange at the transmitter (44)

and non-feasibility of OPS beyond a certain distance threshold as explained in Fig. 5(d). Furthermore, the MIMO-CC-CMAC incurs more delay due to the overhead delay due to the negotiation over the common control channel T_{bo} due to the DIFS, SIFS timing interval while transmitting the RTS/CTS packets over the common control channel before the cognitive transmitter and receiver agrees on a particular channel with an assumption that a node will try atleast 5 retransmissions over the control channel before declaring it to be busy and back off for a given duration of time. Fig. 6(f) illustrates the overall interference duration caused to the non-cognitive users for the two access schemes both with MIMO and point-to-point mode of transmission. The MIMO-CC-CMAC will cause minimum interference duration to the non-cognitive users as compared to MIMO-DTS-CMAC and other point to point access schemes because as shown in Fig. 5(d), the OPS value for MIMO-CC-CMAC will be minimum as compared to MIMO-DTS-CMAC and the two other point-to-point access schemes with OPS. Since the average interference duration is dependent on the optimal packet size from (38) therefore, the interference duration for MIMO-CC-CMAC will be minimum.

IX. Conclusion and Future Works

This paper proposed a novel optimal packet size determination framework for MIMO-CRSNs. An optimization model is framed to determine the OPS which apart from determining the OPS, guarantees the minimum energy consumption. Two key algorithms are proposed to evaluate the OPS. From the simulation results it could be seen that the elapsed CPU time for the KKT based Algorithm-2 outperforms Algorithm-1 by a significant margin. The CPU elapsed time for Algorithm-2 is of the order of 5 to 10 ms while for Algorithm-1 it is 600 ms. Although this comparative analysis is shown using MATLAB tool but it is evident from the simulations that then proposed Algorithm-2 would consume much lower execution time and will be a feasible option for real time implementation. Our algorithms is introduced to a centralized common control channel based strategy to compare its performance with the distributed one. In normal scenario, the CSMA/CA assisted centralized common control channel based cognitive access scheme (MIMO-CC-CMAC) with OPS will outperform the distributed (MIMO-DTS-CMAC) with OPS in terms of overall energy consumption. In terms of delay, under unconstrained conditions, MIMO-CC-CMAC will incur additional delay as compared to both MIMO and P2P due to the intracluster overhead. In terms of overall interference duration caused to the non-cognitive users, MIMO-CC-CMAC with OPS causes minimum interference to the non-cognitive users as compared to the MIMO-DTS-CMAC scheme with OPS and other point-to-point schemes. In future more efficient access strategies could be couple with our proposed MIMO-CRSN architecture. Energy harvesting MIMO-CRSN framework with OPS would be an interesting area to which our work could be further extended.

Appendix A
For Subalgorithms- 2.1, 2.2, 2.4 and 2.4

A. Subalgorithm-2.1

$$\frac{\partial \eta}{\partial l_s} = \frac{(1-\overline{P_{eth}})^{M_t l_s}}{(k_1+k_{loc})l_s + Z_3}\left\{M_t k_1 (l_s - M_t h)\log(1-\overline{P_{eth}}) + \frac{Z_5(l_s)}{(k_1+k_{loc})l_s+Z_3}\right\}, \tag{75}$$

where

$$Z_5(l_s) = k_1^{'}(k_{loc}l_s^2 + Z_3 l_s - k_{loc}M_t h l_s) + Z_3(k_1 - M_t h k_1^{'}) + k_1(k_{loc}M_t h + k_1 M_t h) \tag{76}$$

The derivative of k_1 calculated to be as

$$k_1^{'} = (1+\alpha)P_{out}^{'} \tag{77}$$

$$k_1^{'} = (1+\alpha)p_l N_0 \gamma_a^{'} \tag{78}$$

where $p_l = \frac{(4\pi)^2 d_{ss}^{\delta} M_l N_f}{\lambda^2 G_t G_r}$ is the pathloss component.

$$\gamma_a^{'} = \frac{1}{L}\left[\frac{K_a}{\overline{P_{eth}}}\left\{1+\Omega\,(a-1)\right\}\right]^{\frac{1}{L}-1}(a-1)\frac{K_a}{\overline{P_{eth}}}\Omega^{'}(l_s), \tag{79}$$

where

$$a = \left(\frac{N_0 + P_{rp}}{N_0}\right)^L \tag{80}$$

$$K_a = \frac{4}{b}\left(1-\frac{1}{2^{\frac{b}{2}}}\right)\binom{2L-1}{L}\frac{1}{2^L}\left(\frac{3b}{(2^b-1)M_t}\right)^{-L}, \tag{81}$$

$$\Omega'(l_s) = Pr_{on}Pr_{off}\frac{(1-\tilde{P_f})Pr_c\frac{1}{Rv_p}e^{\frac{-l_s}{Rv_p}} - (1-\tilde{P_d})\frac{1}{Rl_p}e^{\frac{-l_s}{Rl_p}}}{Pr_{off}(1-\tilde{P_f}) + Pr_{on}(1-\tilde{P_d})} \tag{82}$$

Based on (75) to (82), the modified cost function $\mathbf{f(l_s)}$ to calculate optimal packet size l_s^{opt} turns out to be

$$\mathbf{f(l_s)} = \left\{M_t k_1 (l_s - M_t h)\log(1-\overline{P_{eth}}) + \frac{Z_5(l_s)}{(k_1+k_{loc})l_s+Z_3}\right\} \tag{83}$$

$$\gamma_a^{''} = K_a(1+(a-1)\Omega(l_s))^{\frac{1}{L}-1}\,\Omega^{''}(l_s) + K_a\left[\Omega^{'}(l_s)\right]^2\left(\frac{1}{L}-1\right)(1+(a-1)\Omega(l_s))^{\frac{1}{L}-2}(a-1) \tag{84}$$

$$Z_5^{'}(l_s) = k_{loc}k_1^{''}l_s^2 + 2k_1^{'}k_{loc}l_s - M_thk_{loc}(k_1^{''}l_s + k_1^{'}) + 2M_thk_1k_1^{'} + M_thk_{loc}k_1^{'} + Z_3(k_1^{''}l_s + 2k_1^{'} - M_thk_1^{''}) \tag{85}$$

$$\mathbf{f}^{''}(\mathbf{l_s}) = 2\log(1-\overline{P_{eth}})(k_1^{'}l_s + k_1 - M_thk_1^{'}) + \left\{ \frac{\{(k_1+k_{loc})l_s + Z_3\}\, Z_5^{'}(l_s) - (k_1^{'}l_s + k_1 + k_{loc})Z_5(l_s)}{\{(k_1+k_{loc})l_s + Z_3\}^2} \right\} \tag{86}$$

$$\Omega''(l_s) = Pr_{on}Pr_{off}\frac{(1-\tilde{P}_d)\frac{1}{(Rl_p)^2}e^{\frac{-l_s}{Rl_p}} - (1-\tilde{P}_f)Pr_c\frac{1}{(Rv_p)^2}e^{\frac{-l_s}{Rv_p}}}{Pr_{off}(1-\tilde{P}_f) + Pr_{on}(1-\tilde{P}_d)}. \tag{87}$$

B. Subalgorithm-2.2

$$c_1^{\mathbf{mimo}^{'}}(l_s, b) = A_1 + l_sB_1, \tag{88}$$

where

$$A_1 = \frac{Pr_{on} + Pr_2Pr_{off}e^{\frac{-l_s}{Rl_p}}}{Pr_2 + Pr_5^{\mathbf{mimo}}} \tag{89}$$

$$B_1 = -\frac{1}{(Pr_2 + Pr_5^{\mathbf{mimo}})^2}\left\{(Pr_2 + Pr_5^{\mathbf{mimo}}) Pr_2Pr_{off}e^{\frac{-l_s}{Rl_p}}\frac{1}{Rl_p} + Pr_2Pr_{off}e^{\frac{-l_s}{Rl_p}}Pr_5^{'\,\mathbf{mimo}}\right\} \tag{90}$$

$$Pr_5^{\mathbf{mimo}^{'}} = \frac{1}{Rv_p}(Pr_{off} - Pr_3 - Pr_4^{\mathbf{mimo}})e^{\frac{-l_s}{Rv_p}} \tag{91}$$

C. Subalgorithm-2.3

$$c_2^{\mathbf{mimo}^{'}}(l_s, b) = 2\frac{M_t\overline{P_{eth}}}{b}l_s + \left(\frac{1}{b} + \frac{1}{b_{loc}} + R_sM_t\overline{P_e}\tau_{tot} - kR_s\right) \tag{92}$$

where

$$A = \frac{M_t\overline{P_{eth}}}{b}, B = \left(\frac{1}{b} + \frac{1}{b_{loc}} + R_sM_t\overline{P_e}\tau_{tot} - kR_s\right) \tag{93}$$

$$C_a = \left(M_thkR_s + \tau_{tot}R_s - \frac{M_th}{b_{loc}}\right) \tag{94}$$

D. Subalgorithm-2.4

$$c_3^{\mathbf{mimo}^{'}}(l_s, b) = \frac{N_0p_l}{M_tL}\left[\frac{K_a}{\overline{P_{eth}}}\{1+\Omega(a-1)\}\right]^{\frac{1}{L}-1}(a-1)\frac{K_a}{\overline{P_{eth}}}\Omega^{'}(l_s), \tag{95}$$

Subalgorithm-2.1 Both delay and interference duration constraints inactive

Require: l_s^{opt}, $c_1^{\mathbf{mimo}}(l_s^{opt})$, $c_2^{\mathbf{mimo}}(l_s^{opt})$, $c_3^{\mathbf{mimo}}(l_s^{opt})$ & k_1^{opt}
Initialize: l_s^*=100, ii=1, $iter$=100, $P_d = \tilde{P}_d = 0.9$, $P_f = \tilde{P}_f = 0.1$ & $\overline{P_e} = \overline{P_{eth}} = 10^{-3}$
while $ii \leq iter$ **do**
  Calculate: • $f(l_s^*)$ & $f^{'}(l_s^*)$, Using (83) and (86)
  • $l_{sa} = l_s^*$
  • $l_s^* = l_s^* - \frac{f(l_s^*)}{f^{'}(l_s^*)}$
  if $|l_{sa} - l_s^*| \leq 10^{-4}$ **then**
    Calculate:
    • $l_s^{opt} \approxeq arg \min_{l_s \in \{\lceil l_s^* \rceil, \lfloor l_s^* \rfloor\}} |l_s - l_s^*|$
    • $c_1^{\mathbf{mimo}}(l_s^{opt})$, $c_2^{\mathbf{mimo}}(l_s^{opt})$, $c_3^{\mathbf{mimo}}(l_s^{opt})$ & k_1^{opt} Using (40), (46), (47) & (70)
    return l_s^{opt}, $c_1^{\mathbf{mimo}}(l_s^{opt})$, $c_2^{\mathbf{mimo}}(l_s^{opt})$,$c_3^{\mathbf{mimo}}(l_s^{opt})$ & k_1^{opt}
  else
    $ii = ii + 1$
  end if
end while

Subalgorithm-2.3 Interference duration constraint inactive and delay constraint active

Require: l_s^{opt}, $c_3^{\mathbf{mimo}}(l_s^{opt})$ & k_1^{opt}
Initialize: $P_d = \tilde{P}_d = 0.9$, $P_f = \tilde{P}_f = 0.1$ & $\overline{P_e} = \overline{P_{eth}} = 10^{-3}$
Calculate: $l_s^{opt1} = \frac{-B+\sqrt{B^2-4AC_a}}{2A}$ $l_s^{opt2} = \frac{-B-\sqrt{B^2-4AC_a}}{2A}$ Using values of A, B & C_a from (92) to (94).
if l_s^{opt1} & l_s^{opt2} is $\Re$ **then**
  if $l_s^{opt1} > l_s^{opt2}$ **then**
    $l_s^{opt1} = \lfloor l_s^{opt1} \rfloor$ $l_s^{opt2} = \lceil l_s^{opt2} \rceil$
  else
    $l_s^{opt2} = \lfloor l_s^{opt2} \rfloor$ $l_s^{opt1} = \lceil l_s^{opt1} \rceil$
  end if
  Calculate: • $\eta^{'}(l_s^{opt1})$, $c_1^{\mathbf{mimo}}(l_s^{opt1})$ & $c_2^{\mathbf{mimo}^{'}}(l_s^{opt1})$
  • $\lambda_{2a} = -\frac{\eta^{'}(l_s^{opt1})}{c_2^{\mathbf{mimo}^{'}}(l_s^{opt1})}$
  • $\eta^{'}(l_s^{opt2})$, $c_1^{\mathbf{mimo}}(l_s^{opt2})$ & $c_2^{\mathbf{mimo}^{'}}(l_s^{opt2})$
  • $\lambda_{2b} = -\frac{\eta^{'}(l_s^{opt2})}{c_2^{\mathbf{mimo}^{'}}(l_s^{opt2})}$
  Using (75) to (82) & (46)
  if $\lambda_{2a} \leq 0$ & $c_1(l_s^{opt1}) \leq 0$ **then**
    $l_s^{opt} = l_s^{opt1}$
    Calculate: $c_3^{\mathbf{mimo}}(l_s^{opt})$ & $k_1(l_s^{opt})$ Using (47), (69) & (70)
    $k_1^{opt} = k_1(l_s^{opt})$
    return l_s^{opt}, $c_3^{\mathbf{mimo}}(l_s^{opt})$ & k_1^{opt}
  else if $\lambda_{2b} \leq 0$ & $c_1(l_s^{opt2}) \leq 0$ **then**
    $l_s^{opt} = l_s^{opt2}$
    Calculate: $c_3^{\mathbf{mimo}}(l_s^{opt})$ & $k_1(l_s^{opt})$ Using (47), (69) & (70)
    $k_1^{opt} = k_1(l_s^{opt})$
    return l_s^{opt}, $c_3^{\mathbf{mimo}}(l_s^{opt})$ & k_1^{opt}
  else
    $l_s^{opt} = \emptyset$, $c_3^{\mathbf{mimo}}(l_s^{opt}) = \emptyset$ & $k_1^{opt} = \emptyset$
  end if
else
  $l_s^{opt} = \emptyset$, $c_3^{\mathbf{mimo}}(l_s^{opt}) = \emptyset$ & $k_1^{opt} = \emptyset$
end if

Subalgorithm-2.2 Interference duration constraint active and delay constraint inactive

Require: l_s^{opt}, $c_3(l_s^{opt})$ & k_1^{opt}
Initialize: $l_s^* = 100$, ii=1, $iter$=100, $P_d = \tilde{P}_d = 0.9$, $P_f = \tilde{P}_f = 0.1$ & $\overline{P_e} = \overline{P_{eth}} = 10^{-3}$
while $ii \leq iter$ **do**
  • $l_{sa} = l_s^*$
  Calculate: • $c_1^{\mathbf{mimo}}(l_s^*)$ & $c_1^{\mathbf{mimo}'}(l_s^*)$ Using (40) and (88)to (91)
  • $l_s^* = l_s^* - \frac{c_1^{\mathbf{mimo}}(l_s^*)}{c_1^{\mathbf{mimo}'}(l_s^*)}$
  if $|l_{sa} - l_s^*| \leq 10^{-4}$ **then**
    $l_s^{opt} = \lfloor l_s^* \rfloor$
    Calculate: • $\eta'(l_s^{opt})$, $c_1^{\mathbf{mimo}'}(l_s^{opt})$, $c_2^{\mathbf{mimo}}(l_s^{opt})$ & $c_3^{\mathbf{mimo}}(l_s^{opt})$
    • $k_1^{opt} = k_1(l_s^{opt})$
    Using (75) to (82), (46), (47), (67) and (70)
    • $\lambda_1 = -\frac{\eta'(l_s^{opt})}{c_1^{\mathbf{mimo}'}(l_s^{opt})}$
    if $\lambda_1 < 0$ & $c_2(l_s^{opt}) \leq 0$ **then**
      return l_s^{opt}, $c_3^{\mathbf{mimo}}(l_s^{opt})$ & k_1^{opt}
    else
      $l_s^{opt} = \emptyset$, $c_3^{\mathbf{mimo}}(l_s^{opt}) = \emptyset$ & $k_1^{opt} = \emptyset$
      return l_s^{opt}, $c_3^{\mathbf{mimo}}(l_s^{opt})$ & k_1^{opt}
    end if
  else if $ii = iter$ **then**
    $l_s^{opt} = \emptyset$, $c_3^{\mathbf{mimo}}(l_s^{opt}) = \emptyset$ & $k_1^{opt} = \emptyset$
    return l_s^{opt}, $c_3^{\mathbf{mimo}}(l_s^{opt})$ & k_1^{opt}
  else
    $ii = ii + 1$
  end if
end while

Subalgorithm-2.4 Transmit power constraint active

Require: l_s^{opt}, $c_3^{\mathbf{mimo}}(l_s^{opt})$ & k_1^{opt}
Initialize: $l_s^* = 100$, $ii = 1$, $iter = 100$
while ii $\leq$ iter **do**
  • $l_{sa} = l_s^*$
  Calculate: • $c_3^{\mathbf{mimo}}(l_s^{opt})$ & $c_3^{\mathbf{mimo}'}(l_s^{opt})$ Using (47) & (95)
  • $l_s^* = l_s^* - \frac{c_3^{\mathbf{mimo}}(l_s^*)}{c_3^{\mathbf{mimo}'}(l_s^*)}$
  if $|l_{sa} - l_s^*| \leq 10^{-4}$ **then**
    $l_s^{opt} = \lfloor l_s^* \rfloor$
    Calculate: • $\eta'(l_s^{opt})$, $c_1^{\mathbf{mimo}}(l_s^{opt})$ & $c_2(l_s^{opt})$
    Using (73), (39) and (46) • $\lambda_3 = -\frac{\eta(l_s^{opt})'}{c_3^{\mathbf{mimo}'}(l_s^{opt})}$
    if $\lambda_3 \leq 0$, $c_1^{\mathbf{mimo}}(l_s^{opt}) \leq 0$ & $c_2(l_s^{opt}) \leq 0$ **then**
      Calculate: k_1^{opt} & $c_3^{\mathbf{mimo}}(l_s^{opt})$ Using (47) and (70)
      return l_s^{opt}, k_1^{opt} & $c_3(l_s^{opt})$
    else
      $l_s^{opt} = \emptyset$, $k_1^{opt} = \emptyset$ & $c_3^{\mathbf{mimo}}(l_s^{opt}) = \emptyset$
      return l_s^{opt}, k_1^{opt} & $c_3(l_s^{opt})$
    end if
  else if $ii = iter$ **then**
    $l_s^{opt} = \emptyset$, $k_1^{opt} = \emptyset$ & $c_3^{\mathbf{mimo}}(l_s^{opt}) = \emptyset$
    return l_s^{opt} , k_1^{opt} & $c_3(l_s^{opt})$
  else
    $ii = ii + 1$
  end if
end while

APPENDIX B
SUBALGORITHMS FOR ALGORITHM-2

REFERENCES

[1] J. Mitola and G. Q. Maguire Jr., "Cognitive radio: making software radios more personal," in IEEE Personal Communications, vol. 6, no. 4, pp.13-18, Aug. 1999.

[2] A. Goldsmith, S. A. Jafar, I. Maric and S. Srinivasa, "Breaking Spectrum Gridlock With Cognitive Radios: An Information Theoretic Perspective," Proc. of the IEEE, vol. 97, no. 5, pp. 894-914, May 2009.

[3] D. T. Otermat, I. Kostanic and C. E. Otero, "Analysis of the FM Radio Spectrum for Secondary Licensing of Low-Power Short-Range Cognitive Internet of Things Devices," *IEEE Access*, vol. 4, no. , pp. 6681-6691, Oct. 2016.

[4] N. u. Hasan, W. Ejaz, S. Lee and H. S. Kim, "Knapsack-based energy-efficient node selection scheme for cooperative spectrum sensing in cognitive radio sensor networks," *IET Commun*., vol. 6, no. 17, pp. 2998-3005, Nov. 27 2012.

[5] G. Vijay, E. B. A. Bdira and M. Ibnkahla, "Cognition in Wireless Sensor Networks: A Perspective," *IEEE Sensors J.*, vol. 11, no. 3, pp. 582-592, Mar 2011.

[6] O. B. Akan, O. Karli, and O. Ergul, "Cognitive radio sensor networks," *IEEE Netw.*, vol. 23, no. 4, pp. 34–40, Aug. 2009.

[7] Y. Sankarasubramaniam, I. F. Akyildiz, and S. W. McLaughlin, "Packet size optimization and its implications on error control for sensor networks,"in Proc. 2003 IEEE Workshop Sensor Netw. Protocols Appl.

[8] S. Kurt; H. U. Yildiz; M. Yigit; B. Tavli; V. C. Gungor, "Packet Size Optimization in Wireless Sensor Networks for Smart Grid Applications," *IEEE Trans. Ind. Electron.*, vol.PP, no.99, pp.1-1, Oct. 2016.

[9] M. C. Oto and O. B. Akan, "Energy-Efficient Packet Size Optimization for Cognitive Radio Sensor Networks," *IEEE Trans. Wireless Commun*., vol. 11, no. 4, pp. 1544-1553, April 2012.

[10] A. Jamal, C. K. Tham and W. C. Wong, "Dynamic Packet Size Optimization and Channel Selection for Cognitive Radio Sensor Networks, "*IEEE Trans. Cognitive Commun. and Netw*., vol. 1, no. 4, pp. 394-405, Dec. 2015.

[11] Chitradeep Majumdar, Doohwan Lee, Aaqib Patel, S. N. Merchant and U. B. Desai, " Packet Size Optimization for Cognitive Radio Sensor Networks aided Internet of Things," *IEEE Access*, vol.PP, no.99, pp.1-1, Oct. 2016.

[12] Shuguang Cui, A. J. Goldsmith, A. Bahai, "Energy-efficiency of MIMO and cooperative MIMO techniques in sensor networks," *IEEE J. Sel. Areas Commun*., vol.22, no.6, pp. 1089-1098, Aug. 2004.

[13] Shuguang Cui, A. J. Goldsmith, A. Bahai, "Energy-constrained modulation optimization," *IEEE Trans. Wireless Commun*., vol.4, no.5, pp. 2349-2360, Sep. 2005.

[14] S. K. Jayaweera, "Virtual MIMO-based cooperative communication for energy-constrained wireless sensor networks,"IEEE Trans. Wireless Commun., vol.5, no.5, pp.984,989, May 2006.

[15] K. Wang and W. Chen, "Energy-Efficient Communications in MIMO Systems Based on Adaptive Packets and Congestion Control With Delay Constraints," *IEEE Trans. Wireless Commun.*, vol. 14, no. 4, pp. 2169-2179, Apr. 2015.

[16] A. Ahmad, S. Ahmad, M. H. Rehmani and N. U. Hassan, "A Survey on Radio Resource Allocation in Cognitive Radio Sensor Networks," *IEEE Commun. Surv. and Tut*., vol. 17, no. 2, pp. 888-917, Secondquarter 2015.

[17] D. Zhang; Z. Chen; M. K. Awad; N. Zhang; H. Zhou; X. S. Shen, "Utility-optimal Resource Management and Allocation Algorithm for Energy Harvesting Cognitive Radio Sensor Networks," *IEEE J. Sel. Areas Commun*., vol.PP, no.99, pp.1-1, Sep. 2016.

[18] H. Gao, W. Ejaz and M. Jo, "Cooperative Wireless Energy Harvesting and Spectrum Sharing in 5G Networks," *IEEE Access*, vol. 4, no. , pp. 3647-3658, Jun. 2016.

[19] D. Zhang; Z. Chen; J. Ren; N. Zhang; M. Awad; H. Zhou; X. Shen, "Energy Harvesting-Aided Spectrum Sensing and Data Transmission in Heterogeneous Cognitive Radio Sensor Network," *IEEE Trans. Veh. Technol*., vol.PP, no.99, pp.1-1, Apr. 2016.

[20] F. Foukalas and T. Khattab, "To Relay or Not to Relay in Cognitive Radio Sensor Networks," *IEEE Trans. Veh. Technol*., vol. 64, no. 11, pp. 5221-5231, Nov. 2015.

[21] G. A. Shah and O. B. Akan, "Cognitive Adaptive Medium Access Control in Cognitive Radio Sensor Networks," *IEEE Trans. Veh. Technol*., vol. 64, no. 2, pp. 757-767, Feb. 2015.

[22] G. A. Shah, F. Alagoz, E. A. Fadel and O. B. Akan, "A Spectrum-Aware Clustering for Efficient Multimedia Routing in Cognitive Radio Sensor Networks," *IEEE Trans. Veh. Technol*., vol. 63, no. 7, pp. 3369-3380, Sept. 2014.

[23] J. Ren, Y. Zhang, N. Zhang, D. Zhang and X. Shen, "Dynamic Channel Access to Improve Energy Efficiency in Cognitive Radio Sensor Networks," *IEEE Trans. Wireless Commun*., vol. 15, no. 5, pp. 3143-3156, May 2016.

[24] G. A. Shah, V. C. Gungor and O. B. Akan, "A Cross-Layer QoS-Aware Communication Framework in Cognitive Radio Sensor Networks for Smart Grid Applications," *IEEE Trans. Indust. Info*., vol. 9, no. 3, pp. 1477-1485, Aug. 2013.

[25] J. Ren, Y. Zhang, Q. Ye, K. Yang, K. Zhang and X. S. Shen, "Exploiting Secure and Energy-Efficient Collaborative Spectrum Sensing for Cognitive Radio Sensor Networks," *IEEE Trans. on Wireless Commun*., vol. 15, no. 10, pp. 6813-6827, Oct. 2016.

[26] M. Monemian and M. Mahdavi, "Analysis of a New Energy-Based Sensor Selection Method for Cooperative Spectrum Sensing in Cognitive Radio Networks," *IEEE Sensors J*., vol. 14, no. 9, pp. 3021-3032, Sep. 2014.

[27] M. Najimi, A. Ebrahimzadeh, S. M. Hosseini Andargoli and A. Fallahi, "Energy-Efficient Sensor Selection for Cooperative Spectrum Sensing in the Lack or Partial Information," IEEE Sensors J., vol. 15, no. 7, pp. 3807- 3818, Jul. 2015.

[28] M. Najimi, A. Ebrahimzadeh, S. M. H. Andargoli, and A. Fallahi, "A novel sensing nodes and decision node selection method for energy efficiency of cooperative spectrum sensing in cognitive sensor

[29] S. Maleki, A. Pandharipande and G. Leus, "Energy-Efficient Distributed Spectrum Sensing for Cognitive Sensor Networks," IEEE Sensors J., vol. 11, no. 3, pp. 565-573, Mar. 2011.

[30] J. Ren; Y. Zhang; R. Deng; N. Zhang; D. Zhang; X. Shen, "Joint Channel Access and Sampling Rate Control in Energy Harvesting Cognitive Radio Sensor Networks," *IEEE Trans. Emerg. Topics in Comput*., vol.PP, no.99, pp.1-1, Apr. 2016.

[31] M. Ozger, E. Fadel and O. B. Akan, M. Ozger, E. Fadel and O. B. Akan, "Event-to-Sink Spectrum-Aware Clustering in Mobile Cognitive Radio Sensor Networks," *IEEE Trans. Mob. Comput*., vol. 15, no. 9, pp. 2221-2233, Sept. 1 2016.

[32] M. Zheng, W. Liang, H. Yu and H. Sharif, "Utility-based opportunistic spectrum access for cognitive radio sensor networks: joint spectrum sensing and random access control," *IET Commun*., vol. 10, no. 9, pp. 1044-1052, 6 9 2016.

[33] P. Spachos and D. Hantzinakos, "Scalable Dynamic Routing Protocol for Cognitive Radio Sensor Networks," *IEEE Sensors J*., vol. 14, no. 7, pp. 2257-2266, July 2014.

[34] R. M. Eletreby, H. M. Elsayed and M. M. Khairy, "Optimal spectrum assignment for cognitive radio sensor networks under coverage constraint," *IET Commun*., vol. 8, no. 18, pp. 3318-3325, 12 18 2014.

[35] S. C. Lin and K. C. Chen, "Improving Spectrum Efficiency via In-Network Computations in Cognitive Radio Sensor Networks," *IEEE Trans. Wireless Commun*., vol. 13, no. 3, pp. 1222-1234, March 2014.

[36] H. Urkowitz, "Energy detection of unknown deterministic signals," Proc. of the IEEE, vol. 55, no. 4, pp. 523-531, Apr. 1967.

[37] Ying-Chang Liang, Yonghong Zeng, E. C. Y. Peh and Anh Tuan Hoang, "Sensing-Throughput Tradeoff for Cognitive Radio Networks," *IEEE Trans. Wireless Commun*., vol. 7, no. 4, pp. 1326-1337, Apr. 2008.

[38] Won-Yeol Lee and I. F. Akyildiz, "Optimal spectrum sensing framework for cognitive radio networks," *IEEE Trans. Wireless Commun*., vol. 7, no. 10, pp. 3845-3857, Oct. 2008.

[39] G. A. Shah, O. B. Akan, G. A. Shah, O. B. Akan, "Performance Analysis of CSMA-based Opportunistic Medium Access Protocol in Cognitive Radio Sensor Networks," Ad Hoc Netw. J. Elsevier., vol. 15, no. 1, pp. 4-13, Jan. 2014.

[40] S. Wang, Wang Yue, J. P. Coon and A. Doufexi, "Energy-Efficient Spectrum Sensing and Access for Cognitive Radio Networks," *IEEE Trans. Veh. Technol*., vol. 61, no. 2, pp.906-912, Feb. 2012.

[41] M. K. Simon and M. Alouini, Digital Communication over Fading Channels. John Wiley & Sons, 2005.

[42] A. Goldsmith, *Wireless Communications*, Cambridge, U.K.: Cambridge Univ. Press, 2005.